Regioselective Addition of Tris(dialkylamino) Phosphines to $[Fe_2(CO)_6(\mu\text{-}PPh_2)\{\mu\text{-}\eta^1\text{:}\eta^2\text{-}(H)C{=}C{=}CH_2\}]$: Novel P−C Coupling Reactions and Unusual Hydrocarbyl Rearrangements

Simon Doherty,*,† Mark Waugh, Tom H. Scanlan, Mark R. J. Elsegood, and William Clegg

Department of Chemistry, Bedson Building, The University of Newcastle upon Tyne, Newcastle upon Tyne, NE1 7RU, U.K.

Received September 9, 1998

Nucleophilic addition of tris(dialkylamino) phosphines, $P(NR_2)_3$ (R = Me or Et, ^{n}Pr), to $[Fe_2(CO)_6(\mu\text{-}PPh_2)\{\mu\text{-}\eta^1\text{:}\eta^2\text{-}(H)C_\alpha{=}C_\beta{=}C_\gamma H_2\}]$ (**1**) affords the dimetallacyclopentene derivatives $[Fe_2(CO)_6(\mu\text{-}PPh_2)(\mu\text{-}\eta^1\text{:}\eta^1\text{-}HC{=}C\{P(NR_2)_3\}CH_2)]$ (R = Me, **2a**; R = Et, **2b**; R = ^{n}Pr, **2c**) or a mixture of the vinylidene- and dimetallacyclobutene-bridged complexes $[Fe_2(CO)_6(\mu\text{-}PPh_2)(\mu\text{-}\eta^1\text{-}C{=}C(CH_3)\{P(NMe_2)_3\})]$ (**3a**) and $[Fe_2(CO)_6(\mu\text{-}PPh_2)(\mu\text{-}\eta^1\text{:}\eta^1\text{-}(CH_3)C{=}C\{P(NMe_2)_3\})]$ (**4a**), respectively, depending upon the reaction conditions. For instance, addition of $P(NR_2)_3$ to an ether solution of $[Fe_2(CO)_6(\mu\text{-}PPh_2)\{\mu\text{-}\eta^1\text{:}\eta^2\text{-}(H)C_\alpha{=}C_\beta{=}C_\gamma H_2\}]$ gave the dimetallacyclopentenes **2a**−**c**, whereas pretreatment of a solution of the allenyl starting material with HBF_4 prior to the addition of $P(NR_2)_3$ gave the vinylidene- and dimetallacyclobutene-bridged products, which co-crystallized as a 67:33 mixture, as determined by single-crystal X-ray crystallography and ^{1}H NMR spectroscopy. We have subsequently shown that the σ−η-allenyl complex $[Fe_2(CO)_6(\mu\text{-}PPh_2)\{\mu\text{-}\eta^1\text{:}\eta^2\text{-}(H)C_\alpha{=}C_\beta{=}C_\gamma H_2\}]$ undergoes a clean and quantitative acid-promoted rearrangement to the σ−η-acetylide-bridged isomer $[Fe_2(CO)_6(\mu\text{-}PPh_2)\{\mu\text{-}\eta^1\text{:}\eta^2\text{-}C{\equiv}CH_3\}]$ (**5**). ^{1}H NMR and deuterium labeling studies suggest that this isomerization occurs via initial protonation at C_γ to afford a kinetic intermediate which rapidly rearranges to its thermodynamically more stable propyne-bridged counterpart followed by deprotonation. Clearly, the vinylidene and dimetallacyclobutene products isolated from the reaction between **1** and tris(dialkylamino) phosphine in the presence of acid arise from nucleophilic addition to the α- and β-carbon atoms of the acetylide bridge in $[Fe_2(CO)_6(\mu\text{-}PPh_2)\{\mu\text{-}\eta^1\text{:}\eta^2\text{-}C{\equiv}CCH_3\}]$, and not from nucleophilic addition followed by hydrogen migration. In refluxing toluene, the dimetallacyclopentenes $[Fe_2(CO)_6(\mu\text{-}PPh_2)(\mu\text{-}\eta^1\text{:}\eta^1\text{-}HC{=}C\{P(NR_2)_3\}CH_2)]$ slowly decarbonylate to give $[Fe_2(CO)_5(\mu\text{-}PPh_2)(\mu\text{-}\eta^1\text{:}\eta^3\text{-}C(H)C\{P(NR_2)_3\}CH_2)]$ (R = Me, **6a**; R = Et, **6b**; R = ^{n}Pr, **6c**) bridged by a σ−η^3-coordinated vinyl carbene. In the case of R = Et and ^{n}Pr a competing isomerization also affords the highly unusual zwitterionic α-phosphonium-alkoxide-functionalized σ−σ-alkenyl complex $[Fe_2(CO)_5(\mu\text{-}PPh_2)\{\mu\text{-}\eta^1\text{:}\eta^2\text{-}\{P(NR_2)_3\}C(O)CHC{=}CH_2\}]$ (R = Et, **7b**; R = ^{n}Pr, **7c**), via a $P(NR_2)_3$−carbonyl−allenyl coupling sequence. In contrast, isomerization of dimetallacyclopentene $[Fe_2(CO)_6(\mu\text{-}PPh_2)(\mu\text{-}\eta^1\text{:}\eta^1\text{-}HC{=}C\{PPh_3\}CH_2)]$ (**8**) to its σ−η-alkenyl counterpart $[Fe_2(CO)_5(\mu\text{-}PPh_2)\{\mu\text{-}\eta^1\text{:}\eta^2\text{-}PPh_3C(O)CHC{=}CH_2\}]$ (**9**) is essentially complete within 1 h at room temperature with no evidence for the formation of the corresponding vinyl carbene. Thermolysis of a toluene solution of **8** in the presence of excess $P(NEt_2)_3$ results in exclusive formation of **7b**, whereas at room temperature phosphine substitution affords **2b**, via PPh_3−$P(NEt_2)_3$ exchange. The isomerization of **8** to **9** and **2b**,**c** to **7b**,**c** appears to involve a dissociative equilibrium between the kinetic regioisomeric intermediate dimetallacyclopentene and **1**, nucleophilic attack of phosphine at a carbonyl ligand of **1** to give a zwitterionic acylate intermediate, followed by acyl−allenyl coupling to afford the thermodynamically favored zwitterionic σ−η-alkenyl derivative. Qualitatively, the rate of isomerization increases as the steric bulk of the phosphine increases, in the order $P(NMe_2)_3 < P(NEt_2)_3 \approx P(N^nPr_2)_3 < PPh_3$. The single-crystal X-ray structures of **2a**, **3a**, **4a**, **6b**, **7b**, **8**, and **9** are reported.

Introduction

A thorough and detailed examination of the reactivity of mono- and binuclear allenyl (−C(H)=C=CH_2) and propargyl (−CH_2C≡CH) complexes has revealed a varied and exciting organometallic chemistry for this C_3 fragment.[1] A number of these transformation are particularly relevant to organic synthesis such as the Lewis acid-mediated [3+2] cycloaddition reactions of tungsten

† E-mail: simon.doherty@newcastle.ac.uk.

10.1021/om980757n CCC: $18.00
Publication on Web 01/26/1999

propargyl derivatives with aldehydes to give η^1-2,5-dihydro-3-furyl-based products,[2] the formation of five-, six-, and seven-membered lactone rings via tungsten-promoted cyclocarbonylation reactions,[3] the synthesis of α-methylene butyrolactones via the alkoxycarbonylation of molybdenum and tungsten compounds,[4] the synthesis of indanones and unsaturated carbonyl compounds via oxidative carbonylation of tungsten propargyl derivatives,[5] and the titanium-mediated synthesis of allenyl and homopropargyl alcohols.[6] In addition, the fundamental reactivity of mononuclear η^3- and binuclear $\sigma-\eta^2$-coordinated propargyl and allenyl ligands has attracted considerable academic interest, and numerous examples of unusual reactivity patterns have been reported.[1] While the reactivity of mononuclear cationic transition metal allenyl complexes has been well documented, dominated largely by the generation of central carbon-substituted allyl derivatives via regiospecific addition of nucleophiles to the central carbon atom,[7] the reaction chemistry of binuclear allenyl complexes is far more diverse. For instance, examples of nucleophilic addition to the central and both terminal allenylic carbon atoms are commonplace[8] and, more recently, reports of nucleophile−carbonyl−allenyl coupling involving alkyllithium reagents,[9] amines,[10] and alcohols,[11] a diphosphine-promoted migratory insertion−elimination,[12] and a host of obscure ligand coupling reactions.[13]

In the case of neutral phosphorus-based nucleophiles various reaction pathways are possible, the two most common of which are carbonyl substitution and addition to the coordinated hydrocarbon.[14] In this regard, we have recently begun to investigate the reactivity of the diiron allenyl complex $[Fe_2(CO)_6(\mu\text{-}PPh_2)\{\mu\text{-}\eta^1\text{:}\eta^2\text{-}(H)C_\alpha{=}C_\beta{=}C_\gamma H_2\}]$ (**1**) and discovered an unprecedented nucleophilic attack of diphenylphosphine at C_α to afford the phosphino-substituted $\mu\text{-}\eta^1\text{:}\eta^2$-alkenyl complex $[Fe_2(CO)_6(\mu\text{-}PPh_2)\{\mu\text{-}\eta^1\text{:}\eta^2\text{-}CH_3C{=}CH(PPh_2)\}]$.[8b] Mono- and bidentate tertiary phosphines also undergo regiospecific $P-C_\alpha$ bond formation with **1**. For instance, reaction with bis(diphenylphosphino)methane results in $P-C_\alpha$ bond formation and C−H activation to give $[Fe_2(CO)_6(\mu\text{-}PPh_2)\{\mu\text{-}\eta^1(P)\text{:}\eta^1(C)\text{:}\eta^2(C)\text{-}Ph_2PCHPPh_2(H)C{=}CCH_3\}]$, which contains an unusual iron−carbon-bridged phosphinomethanide.[15] In contrast, monodentate trialkyl phosphites undergo $P-C_\alpha$ bond formation and electrophilic induced dealkylation to give the α,β-unsaturated phosphonates $[Fe_2(CO)_6(\mu\text{-}PPh_2)(\mu\text{-}\eta^1\text{:}\eta^2\text{-}CH_3C{=}CCH\{PO(OR)_2\})]$ via either an Arbuzov-type mechanism or direct nucleophilic attack of water on the phosphorus atom of a zwitterionic phosphonium intermediate.[16] As part of our ongoing investigations, we reasoned that the addition of tris(dialkylamino) phosphines, $P(NR_2)_3$ (R = Me, Et, ^{n}Pr), to **1** would only give the corresponding α,β-unsaturated phosphonates via the hydrolysis route since Arbuzov-type dealkylation would be unfavorable.[17]

(1) (a) Wojcicki, A. *New J. Chem*. **1994**, *18*, 61. (b) Doherty, S.; Corrigan, J. F.; Carty, A. J.; Sappa, E. *Adv. Organomet. Chem*. **1995**, *37*, 39.

(2) (a) Shui, H.-G.; Shui, L.-H.; Wang, S.-H.; Wang, S.-L.; Lee, G.-H.; Peng, S.-M.; Lui, R.-S. *J. Am. Chem. Soc*. **1996**, *118*, 530. (b) Wang, S.-H.; Shui, L.-H.; Shui, H.-G.; Liao, Y.-L.; Wang, S.-L.; Lee, G.-H.; Peng, S.-M.; Lui, R.-S. *J. Am. Chem. Soc*. **1994**, *116*, 5967.

(3) Chen, C.-C.; Fan, J.-S.; Lee, G.-H.; Peng, S.-M.; Wang, S.-L.; Liu, R.-S. *J. Am. Chem. Soc*. **1995**, *117*, 2933.

(4) (a) Shieh, S.-J.; Liu, R.-S. *Tetrahedron Lett*. **1997**, *38*, 5209. (b) Shieh, S.-J.; Chen, C.-C.; Liu, R.-S. *J. Org. Chem*. **1997**, *62*, 1986. (c) Shieh, S.-J.; Tang, T.-C.; Lee, J.-S.; Lee, G.-H.; Peng, S.-M.; Liu, R.-S. *J. Org. Chem*. **1996**, *61*, 3245. (d) Chen, C.-C.; Fan, J.-S.; Shieh, S.-J.; Lee, G.-H.; Peng, S.-M.; Wang, S.-L.; Liu, R.-S. *J. Am. Chem. Soc*. **1996**, *118*, 9279.

(5) Liang, K. W.; Chandrasekharam, M.; Li, C. L.; Liu, R. S. *Organometallics* **1998**, *17*, 2683.

(6) Nakagawa, T.; Kasatkin, A.; Sato, F. *Tetrahedron Lett*. **1995**, *36*, 3207.

(7) For a selection of recent examples see: (a) Chen, J.-T.; Hsu, R.-H.; Chen, A.-J. *J. Am. Chem. Soc*. **1998**, *1120*, 3243. (b) Casey, C. P.; Yi, C.-S. *J. Am. Chem. Soc*. **1992**, *114*, 6597. (c) Casey, C. P.; Nash, J. R.; Yu, C. S.; Selmeczy, A. D.; Chung, S.; Powell, D. R.; Hayashi, R. K. *J. Am. Chem. Soc*. **1998**, *120*, 722. (d) Tsutsumi, K.; Ogoshi, S.; Nishigushi, S.; Kurosawa, H. *J. Am. Chem. Soc*. **1998**, *120*, 1938. (e) Baize, M.; Blosser, P. W.; Plantevin, V.; Schimpff, D. G.; Gallucci, J. C.; Wojcicki, A. *Organometallics* **1996**, *15*, 164. (f) Plantevin, V.; Blosser, P. W.; Gallucci, J. C.; Wojcicki, A. *Organometallics* **1994**, *13*, 3651. (g) Blosser, P. W.; Schimpff, D. G.; Gallucci, J. C.; Wojcicki, A. *Organometallics* **1993**, *12*, 1992. (h) Baize, M.; Plantevin, V.; Gallucci, J. C.; Wojcicki, A. *Inorg. Chim. Acta* **1995**, *235*, 1. (i) Hsu, R.-H.; Chen, J.-T.; Lee, G.-H.; Wang, Y. *Organometallics* **1997**, *16*, 1159. (j) Chen, J.-T.; Chen, Y.-K.; Hu, J.-B.; Lee, S.-H.; Wang, Y. *Organometallics* **1997**, *16*, 1476. (k) Tsai, F. Y.; Chen, H. W.; Chen, J. T.; Lee, G. H.; Wang, Y. *Organometallics* **1997**, *16*, 822. (l) Huang, T.-M.; Hsu, R.-H.; Yang, C.-S.; Chen, J.-T.; Lee, G.-H.; Wang, Y. *Organometallics* **1994**, *13*, 3657. (m) Huang, T.-M.; Hsu, R.- H.; Yang, C.-S.; Chen, J.-T.; Lee, G.-H.; Wang, Y. *Organometallics* **1994**, *13*, 3577. (n) Chen, C.-C.; Fan, J.-S.; Lee, G.-H.; Peng, S.-M.; Wang, S.-L.; Lui, R.-S. *J. Am. Chem. Soc*. **1995**, *117*, 2933. (o) Huang, T.-M.; Chen, J.-T.; Lee, G.-H.; Wang, Y. *J. Am. Chem. Soc*. **1993**, *115*, 1170. (p) Su, C.-C.; Chen, J.-T.; Lee, G.-H.; Wang, Y. *J. Am. Chem. Soc*. **1994**, *116*, 4999.

(8) (a) Breckenridge, S. M.; Taylor, N. J.; Carty, A. J. *Organometallics* **1991**, *10*, 837. (b) Doherty, S.; Elsegood, M. R. J.; Clegg, W.; Scanlan, T. H.; Rees, N. H. *Chem. Commun*. **1996**, 1545. (c) Meyer, A.; McCabe, D. J.; Curtis, M. D. *Organometallics* **1987**, *6*, 1491. (d) McLain, M. D.; Hay, M. S.; Curtis, M. D.; Kampf, J. W. *Organometallics* **1994**, *13*, 4377. (e) Henrick, K.; McPartlin, M.; Deeming, A. J.; Hasso, S.; Manning, P. *J. Chem. Soc., Dalton Trans*. **1982**, 899. (f) Amouri, H.; Besace, Y.; Vaissermann, J.; Ricard, L. *Organometallics* **1997**, *16*, 2160. (g) Bradley, D. H.; Khan, M. A.; Nicholas, K. M. *Organometallics* **1992**, *11*, 2598. (h) Caffyn, A. M.; Nicholas, K. M. *J. Am. Chem. Soc*. **1993**, *115*, 6438.

(9) Doherty, S.; Elsegood, M. R. J.; Clegg, W.; Rees, N. H.; Scanlan, T. H.; Waugh, M. *Organometallics* **1997**, *16*, 3221.

(10) (a) Doherty, S.; Hogarth, G.; Elsegood, M. R. J.; Clegg, W.; Rees, N. H.; Waugh, M. *Organometallics* **1998**, *17*, 3331. (b) Doherty, S.; Elsegood, M. R. J.; Clegg, W.; Waugh, M. *Organometallics* **1996**, *15*, 2688.

(11) Doherty, S.; Elsegood, M. R. J.; Clegg, W.; Mampe, D. *Organometallics* **1997**, *16*, 1186.

(12) Blenkiron, P.; Corrigan, J. F.; Taylor, N. J.; Carty, A. J.; Doherty, S.; Elsegood, M.; Clegg, W. *Organometallics* **1997**, *16*, 297.

(13) (a) Blenkiron, P.; Breckenridge, S. M.; Taylor, N. J.; Carty, A. J.; Pellinghelli, M. A.; Tiripicchio, A.; Sappa, E. *J. Organomet. Chem*. **1996**, *506*, 229. (b) Carleton, N.; Corrigan, J. F.; Doherty, S.; Pixner, R.; Sun, Y.; Taylor, N. J.; Carty, A. J. *Organometallics* **1994**, *13*, 4179. (c) Breckenridge, S. M.; Carty, A. J. Pellinghelli, M. A.; Tiripicchio, A.; Sappa, E. *J. Organomet. Chem*. **1994**, *471*, 211. (d) Ogoshi, S.; Tsutsumi, K.; Ooi, M.; Kurosawa, H. *J. Am. Chem. Soc*. **1995**, *117*, 10415.

(14) For addition to a coordinated organic ligand see: (a) Takats, J.; Washington, L.; Santarsiero, B. D. *Organometallics* **1994**, *13*, 1078. (b) Slugovc, C.; Mauthner, K.; Mereiter, K.; Schmid, R.; Kirchner, K. *Organometallics* **1996**, *15*, 2954. (c) Seyferth, S.; Hoke, J. B.; Wheeler, D. R. *J. Organomet. Chem*. **1988**, *341*, 421. (d) Boyar, E.; Deeming, A. J.; Kabir, S. E. *J. Chem. Soc., Chem. Commun*. **1986**, 577. (e) Deeming, A. J.; Hasso, S. J. *Organomet. Chem*. **1976**, *112*, C39. (f) Deeming, A. J.; Manning, P. *J. Organomet. Chem*. **1984**, *265*, 87. (g) Kreissl, F. R.; Hel, W. *Chem. Ber*. **1977**, *110*, 799. (h) Fischer, E. O.; Reitmeier, R.; Ackermann, K. *Angew. Chem., Int. Ed. Engl*. **1983**, *22*, 411. (i) Kreissl, F. R.; Friedrich, P. *Angew. Chem., Int. Ed. Engl*. **1977**, *16*, 543. (j) Kreissl, F. R.; Stuckler, P.; Meineke, E. W. *Chem. Ber*. **1977**, *110*, 3040. (k) Fischer, E. O.; Ruhs, A.; Kreissl, F. R. *Chem. Ber*, **1977**, *110*, 805. (l) Busetto, L.; Carlucci, L.; Zanotti, V.; Albano, V. G.; Monari, M. *Chem. Ber*. **1992**, *125*, 1125. (m) Bassi, M.; Carlucci, L.; Zanotti, V. *Inorg. Chim. Acta*. **1993**, *204*, 171. (n) Henrick, K.; McPartlin, M.; Deeming, A. J.; Hasso, S.; Manning, P. *J. Chem. Soc., Dalton Trans*. **1982**, 899. (o) For carbonyl substitution reactions see: Darensbourg, D. J. In *The Chemistry of Metal Cluster Complexes*; Shriver, D. F., Keasz, H. D., Adams, R. D., Eds.; VCH: New York, 1990; Chapter 4. Poe, A. J. In *Metal Clusters*; Moskovits, M., Ed.; Wiley-Interscience: New York, 1986; Chapter 4. Chen, L. Z.; Poe, A. L. *Coord. Chem. Rev*. **1995**, *143*, 265.

(15) Doherty, S.; Elsegood, M. R. J.; Clegg, W.; Mampe, D. *Organometallics* **1996**, *15*, 5302.

(16) Doherty, S.; Elsegood, M. R. J.; Clegg, W.; Ward, M. F. W.; Waugh, M. *Organometallics* **1997**, *16*, 4251.

Scheme 1

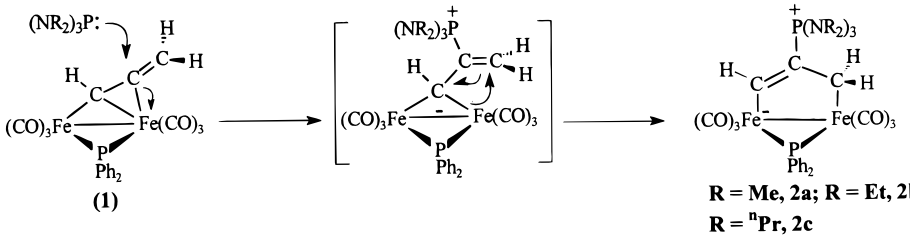

However, these studies have been inconclusive since tris(dialkylamino) phosphines do not add to C_α but preferentially add to C_β, to give the dimetallacyclopentene derivatives $[Fe_2(CO)_6(\mu\text{-}PPh_2)(\mu\text{-}\eta^1\text{:}\eta^1\text{-}HC{=}C\{P(NR_2)_3\}CH_2)]$. Herein we report the results of these investigations and highlight a number of noteworthy features associated with the chemistry of dimetallacyclopentenes including (i) the facile decarbonylation of $[Fe_2(CO)_6(\mu\text{-}PPh_2)(\mu\text{-}\eta^1\text{:}\eta^1\text{-}HC{=}C\{P(NR_2)_3\}CH_2)]$ to give $[Fe_2(CO)_5(\mu\text{-}PPh_2)(\mu\text{-}\eta^3\text{-}C(H)C\{P(NR_2)_3\}CH_2)]$, bridged by a $\sigma\text{−}\eta$-coordinated vinyl carbene, (ii) the acid-promoted isomerization of the $\sigma\text{−}\eta$-allenyl ligand into a $\sigma\text{−}\eta$-acetylide, (iii) the formation of a dissociative equilibrium between **1** and $[Fe_2(CO)_6(\mu\text{-}PPh_2)(\mu\text{-}\eta^1\text{:}\eta^1\text{-}HC{=}C\{PR_3\}CH_2)]$ (R = NEt_2, N^nPr_2, Ph), and (iv) isomerization of the dimetallacyclopentene $[Fe_2(CO)_6(\mu\text{-}PPh_2)(\mu\text{-}\eta^1\text{:}\eta^1\text{-}HC{=}C\{PR_3\}CH_2)]$ to $[Fe_2(CO)_5(\mu\text{-}PPh_2)\{\mu\text{-}\eta^1\text{:}\eta^2\text{-}\{PR_3\}C(O)CHC{=}CH_2\}]$, via PR_3 dissociation and a highly unusual phosphine−carbonyl−allenyl coupling sequence.

Results and Discussion

Synthesis of $[Fe_2(CO)_6(\mu\text{-}PPh_2)(\mu\text{-}\eta^1\text{:}\eta^1\text{-}HC{=}C\{P(NR_2)_3\}CH_2)]$ (R = Me, 2a; R = Et, 2b; R = ^{n}Pr, 2c). Addition of $P(NR_2)_3$ (R = Me, Et, ^{n}Pr$_2$) to a solution of $[Fe_2(CO)_6(\mu\text{-}PPh_2)\{\mu\text{-}\eta^1\text{:}\eta^2\text{-}(H)C_\alpha{=}C_\beta{=}C_\gamma H_2\}]$ (**1**) in diethyl ether results in a gradual color change from orange to yellow and the formation of the zwitterionic dimetallacyclopentene derivatives $[Fe_2(CO)_6(\mu\text{-}PPh_2)(\mu\text{-}\eta^1\text{:}\eta^1\text{-}HC{=}C\{P(NR_2)_3\}CH_2)]$ (R = Me, **2a**; R = Et, **2b**; R = ^{n}Pr$_2$, **2c**), which can be isolated as yellow crystalline solids in up to 70−80% yield (Scheme 1).

The formation of **2a**−**c** involves regioselecive P−C bond formation to C_β of the allenyl ligand in **1**, presumably via an alkylidene-bridged intermediate that rapidly undergoes a 1,3-shift of iron to the terminal methylene carbon. This in itself is an interesting transformation since our previous studies have shown that mono- and bidentate phosphorus-based nucleophiles react with **1** via addition to C_α to generate a range of P-functionalized unsaturated-hydrocarbyl bridging ligands.[8b,15,16] Notably though, selected primary amines react with **1** via addition to the central allenylic carbon with proton transfer to C_α to afford closely related dimetallacyclopentane derivatives.[10a] The ^{1}H and ^{13}C spectroscopic properties of **2a**−**c** are consistent with the dimetallacyclopentene structure shown in Scheme 1. In particular, in the ^{1}H NMR spectrum the three protons attached to the C_3 bridging hydrocarbon appear as distinct resonances, the methine proton typically in the low-field region ($\delta \sim 7.85$) and the methylene protons at much higher field ($\delta \sim 1.09$). In the $^{13}C\{^1H\}$ NMR spectrum a high-field doublet at δ 190.2 (**2a**, $^2J_{PC}$ = 18.1 Hz), 187.3 (**2b**, $^2J_{PC}$ = 17.7 Hz), and 188.0 (**2c**, $^2J_{PC}$ = 16.6 Hz) is suggestive of carbene-like character in the Fe−C_α bond.[18] The resonance associated with the central carbon atom of **2a** appears at δ 136.9 and is strongly coupled to the tris(dimethylamino) phosphine phosphorus atom ($^1J_{PC}$ = 92.0 Hz) and weakly coupled to the phosphorus atom of the phosphido bridge ($^3J_{PC}$ = 16.0 Hz). The remaining carbon atom of the C_3 bridge in **2a** gives rise to a doublet at δ 17.1 ($^2J_{PC}$ = 14.0 Hz) and is in the region expected for C_γ of a dimetallacyclopentene derivative, which generally lies at much higher field than C_α and C_β.[18] The $^{31}P\{^1H\}$ NMR spectrum of **2a** is unexceptional and serves to confirm the presence of a carbon-bound $P(NMe_2)_3$ and a phosphido ligand that bridges an Fe−Fe bond.[19] On the basis of this data we are confident that **2a**−**c** correspond to the dimetallacyclopentenes $[Fe_2(CO)_6(\mu\text{-}PPh_2)(\mu\text{-}\eta^1\text{:}\eta^1\text{-}HC{=}C\{P(NR_2)_3\}CH_2)]$ (R = Me, **2a**; R = Et, **2b**; R = ^{n}Pr$_2$, **2c**). However, since these are the first zwitterionic dimetallacyclopentene derivatives of iron to be characterized, a single-crystal X-ray structure determination of **2a** was undertaken to provide precise details of the metal−ligand bonding.

A perspective view of the molecular structure, together with the atomic numbering scheme, is shown in Figure 1, and selected bond lengths and angles are listed in Table 1. The molecular structure clearly shows the C_3-hydrocarbyl fragment σ-bonded via C(1) to Fe(1) (Fe(1)−C(1) = 2.042(4) Å) and via C(3) to Fe(2) (Fe(2)−C(3) = 2.060(4) Å). The carbon−carbon bond length of 1.379(6) Å for C(1)−C(2) is typical for an olefinic C(sp^2)−C(sp^2) double bond, while a distance of 1.446(6) Å for C(2)−C(3) is close to that expected for a C(sp^2)−C(sp^3) single bond. The five-membered Fe_2C_3 ring is remarkably planar (mean deviation from plane = 0.031 Å) and is essentially perpendicular to the phosphido bridge (angle between planes Fe(1), Fe(2), P(2) and Fe(1), Fe(2), C(1), C(2), C(3) = 90.3°). The planarity at C(2) (sum of angles 359.8°), the Fe(1)−C(1) distances of 2.042(4) Å, and the Fe(2)−C(3) distance of 2.060(4) Å confirm that **2a** is largely metallacyclopentene with negligible contribution from the carbene−phosphorus ylide resonance structure.[18] As expected the two iron atoms are within bonding distance (Fe(1)−Fe(2) = 2.7140(9) Å), asymmetrically bridged by the phosphido ligand (Fe(1)−P(2)

(17) (a) Yu, Y.; Jablonski, C.; Bridson, J. *Organometallics* **1997**, *16*, 1270. (b) Nakazawa, H.; Ueda, Y.; Nakamura, K.; Miyoshi, K. *Organometallics* **1997**, *16*, 1562.

(18) Cherkas, A. A.; Breckenridge, S. M.; Carty, A. J. *Polyhedron* **1992**, *11*, 1075.

(19) (a) Carty, A. J.; MacLaughlin, S. A.; Nicciarone, D. *In Phosphorus-31 NMR Spectroscopy in Stereochemical Analysis: Organic Compounds and Metal Complexes*; Verkade, J. G., Quinn, L. D., Eds.; VCH: New York, 1987; Chapter 16, pp 54−619. (b) Carty, A. J. *Adv. Chem Ser.* **1982**, *196*, 163.

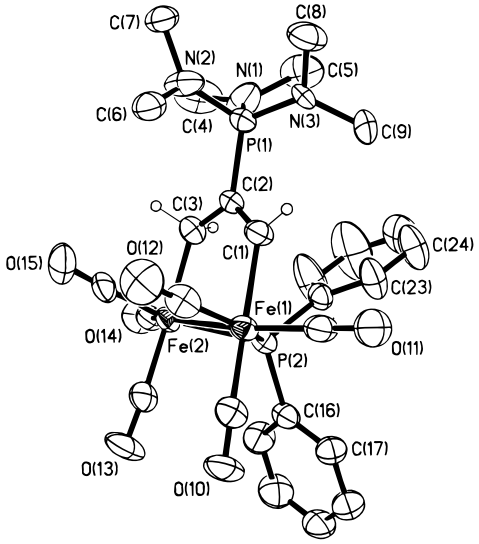

Figure 1. Molecular structure of $[Fe_2(CO)_6(\mu\text{-}PPh_2)(\mu\text{-}\eta^1\text{:}\eta^1\text{-}HC{=}C\{P(NMe_2)_3\}\text{-}CH_2)]$ (**2a**). Phenyl and hydrogen atoms have been omitted. Carbonyl carbons have the same numbers as oxygen atoms. Ellipsoids are at the 50% probability level.

Table 1. Selected Bond Distances (Å) and Angles (deg) for Compound 2a

Fe(1)−Fe(2)	2.1740(9)	Fe(1)−C(1)	2.042(4)
Fe(2)−C(3)	2.060(4)	C(1)−C(2)	1.379(6)
C(2)−C(3)	1.446(6)	C(2)−P(1)	1.783(4)
Fe(1)−P(2)	2.1813(13)	Fe(2)−P(2)	2.1920(13)
C(1)−C(2)−C(3)	125.0(4)	C(1)−C(2)−P(1)	117.9(3)
C(3)−C(2)−P(1)	116.9(3)	Fe(1)−P(2)−Fe(2)	76.72(4)
C(3)−Fe(2)−P(2)	87.62(13)	P(2)−Fe(1)−C(1)	88.50(13)

= 2.1813(13); Fe(2)−P(2) = 2.1920(13) Å) and both carrying three mutually cis carbonyl ligands, which are eclipsed with respect to each other.

Synthesis of $[Fe_2(CO)_6(\mu\text{-}PPh_2)(\mu\text{-}\eta^1\text{-}C{=}C(CH_3)\{P(NMe_2)_3\})]$ (3a) and $[Fe_2(CO)_6(\mu\text{-}PPh_2)(\mu\text{-}\eta^1\text{:}\eta^1\text{-}(CH_3)C{=}C\{P(NMe_2)_3\})]$ (4a). In contrast to the formation of **2a**−**c** described above, pretreatment of a solution of **1** with HBF_4 prior to addition of $P(NMe_2)_3$ gave a mixture of the vinylidene-bridged complex $[Fe_2(CO)_6(\mu\text{-}PPh_2)(\mu\text{-}\eta^1\text{-}C{=}C(CH_3)\{P(NMe_2)_3\})]$ (**3a**) and the dimetallacyclobutene $[Fe_2(CO)_6(\mu\text{-}PPh_2)(\mu\text{-}\eta^1\text{:}\eta^1\text{-}(CH_3)C{=}C\{P(NMe_2)_3\})]$ (**4a**), which were not separable by TLC or column chromatography (Scheme 2). Moreover, even after repeated crystallization **3a** and **4a** were consistently isolated in the same 67:33 ratio, as determined by ^1H NMR spectroscopy and X-ray crystallography (vide infra). The major product, **3a**, has a three-proton doublet of doublets at δ 2.07 ($^3J_{PH}$ = 3.65 Hz, $^5J_{PH}$ = 0.8 Hz) for the methyl substituent of the bridging vinylidene and an 18-proton doublet at δ 2.28 ($^3J_{PH}$ = 9.15 Hz) associated with the carbon-bound $P(NMe_2)_3$ group. In the $^{13}C\{^1H\}$ spectrum of **3a** resonances at δ 200.9 and 111.2 fall within the range of chemical shifts for C_α and C_β in μ_2-vinylidene complexes.[20] In the $^{13}C\{^1H\}$ NMR spectrum of **4a** a signal at δ 115.6 is in the range expected for a parallel acetylene complex[21] and strongly coupled to the phosphorus atom of the tris(dimethylamino) phosphine ($^1J_{PC}$ = 142.0 Hz) and only weakly coupled to the phosphorus atom of the phosphido bridge ($^2J_{PC}$ = 2.4 Hz). The resonance for the remaining carbon atom of the C_2 bridge is further downfield at δ 219.4 and shows a larger coupling constant to the phosphido bridge phosphorus atom ($^2J_{PC}$ = 15.8 Hz), which suggests more carbene-like character for this carbon atom than for that at δ 115.6.[18]

To establish precise details of the structures of these two isomers, an X-ray crystallographic study was undertaken. Complexes **3a** and **4a** co-crystallize in the space group $P2_1$ with a 66.8(11):33.2(11)% occupancy. The iron, methyl, and $P(NMe_2)_3$ groups are common to both components. Perspective views of the molecular structures of **3a** and **4a** are shown in Figures 2 and 3, respectively, and selected bond lengths and angles for both molecules are given in Table 2. For clarity and distinction the structures of **3a** and **4a** are described separately. In **3a** the two iron atoms are bonded by a strong metal−metal interaction (Fe(1)−Fe(2) = 2.5767(11) Å) and asymmetrically bridged by the phosphorus atom of a bridging phosphido group (Fe(1)−P(2) = 2.1886(15) Å; Fe(2)−P(2) = 2.048(14) Å) as well as a one-atom asymmetrically bridging vinylidene ligand (Fe(1)−C(1) = 1.997(10) Å; Fe(2)−C(1) = 1.838(8) Å). While the Fe(1)−C(1) bond length is in the range expected for a diiron−vinylidene structure, the Fe(2)−C(1) bond is slightly shorter than previously reported values, which typically lie in the range 1.874−1.969 Å.[20] The C(1)−C(2) bond length of 1.350(13) Å is typical of C=C bond distances in diiron μ_2-vinylidene-bridged complexes, which are generally between 1.266 and 1.358 Å, and close to that expected for a $C(sp^2)-C(sp^2)$ bond length.[22] As expected for a vinylidene-bridged dimer, C(2) is essentially sp^2 in nature, since all the angles at this carbon are close to 120° (∠C(1)C(2)C(3) = 118.5(7)°, ∠C(1)C(2)P(1) = 121.4(8)°, ∠C(3)C(2)P(1) = 120.1(6)°). Although formally sp^2, C(1) is severely distorted from the ideal trigonal geometry, with angles of 126.4(7)°, 84.3(4)°, and 149.0(5)°. The short Fe−Fe bond and acute FePFe angle of 71.82(5)° is the result of the one-atom hydrocarbyl bridging group.[23] The P(1)−C(2) bond length of 1.734(8) Å is substantially shorter than that of 1.8257(16) Å in **6a** (vide infra) and, together with the asymmetry in the vinylidene−iron bridge, suggests that P(1), C(2), C(1), Fe(2) is partially delocalized with contributions from resonance structures **I** and **II** in Chart 1. The vinylidene bond C(1)−C(2) shows only a small rotation such that the dihedral angle between the planes formed by P(1), C(3), C(2), and C(1) and Fe(2), Fe(1), C(1), and C(2) is 7.5° and the small angle subtended by the metal atoms at the μ-C=CRR′ bridge (84.3(4)°) is characteristic of a binuclear vinylidene complex.

The molecular structure shown in Figure 3 identifies the second compound in the crystal as the dimetalla-

(20) (a) Bruce, M. I. *Chem. Rev.* **1991,** *91*, 250. (b) Randall, L. H.; Breckenridge, S. M.; Hogarth, G.; Cleroux, M.; Doherty, S.; Cherkas, A. A.; Taylor, N. J.; Carty, A. J. *Organometallics* **1992**, *11*, 1701.

(21) (a) Wong, Y.-S.; Paik, H. N.; Chieh, P. C.; Carty, A. J.; Mott, G. N.; Taylor, N. J. *J. Organomet. Chem.* **1981**, *212*, C54. (b) Johnson, K. A.; Gladfelter, W. L. *Organometallics* **1989**, *8*, 2866. (c) Burn, M. J.; Keil, G. Y.; Seils, F.; Takats, J.; Washington, S. *J. Am. Chem. Soc.* **1989**, *111*, 9850.

(22) Bent, H. A. *Chem. Rev.* **1961**, *61*, 275.

(23) (a) Cherkas, A. A.; Hoffman, D.; Taylor, N. J. Carty, A. J. *Organometallics* **1987**, *6*, 1466. (b) Cherkas, A. A.; Mott, G. N.; Granby, R.; MacLaughlin, S. A.; Yule, J. E.; Taylor, N. J.; Carty, A. J. *Organometallics* **1988**, *7*, 1115.

Scheme 2

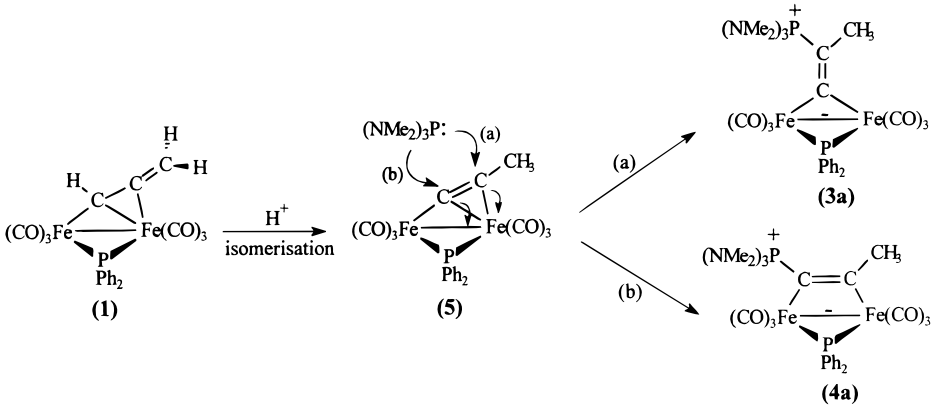

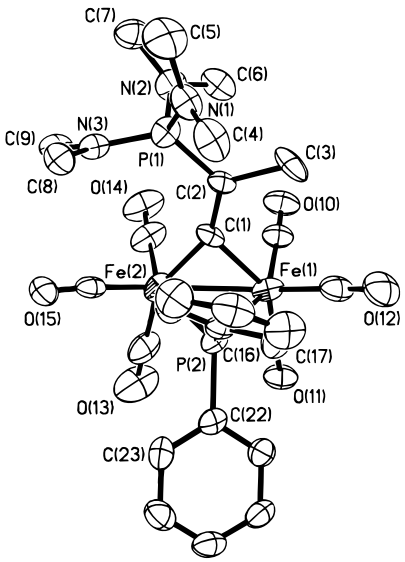

Figure 2. Molecular structure of $[Fe_2(CO)_6(\mu\text{-}PPh_2)(\mu\text{-}\eta^1\text{-}C{=}C(CH_3)\{P(NMe_2)_3\})]$ (**3a**). Phenyl and methyl hydrogen atoms have been omitted. Carbonyl carbons have the same numbers as oxygen atoms. Ellipsoids are at the 50% probability level.

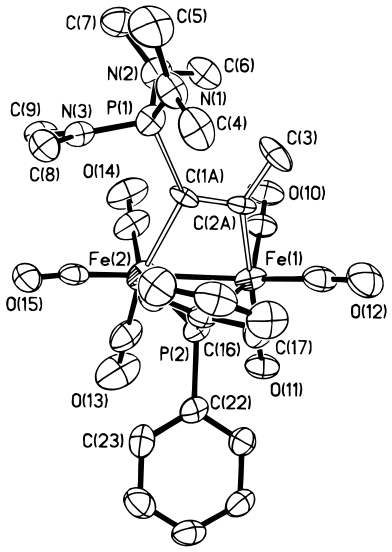

Figure 3. Molecular structure of $[Fe_2(CO)_6(\mu\text{-}PPh_2)(\mu\text{-}\eta^1\text{:}\eta^1\text{-}(CH_3)C{=}C\{P(NMe_2)_3\})]$ (**4a**). Phenyl and methyl hydrogen atoms have been omitted. Carbonyl carbons have the same numbers as oxygen atoms. Ellipsoids are at the 50% probability level.

Chart 1

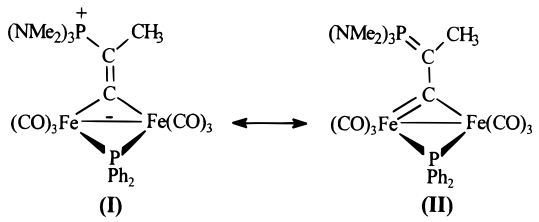

cyclobutene derivative $[Fe_2(CO)_6(\mu\text{-}PPh_2)(\mu\text{-}\eta^1\text{:}\eta^1\text{-}(CH_3)C{=}C\{P(NR_2)_3\})]$ (**4a**), an isomer of **3a** that contains a zwitterionic $\mu\text{-}\eta^1\text{:}\eta^1$-parallel acetylene **III**, formally derived from **1** via allenyl−acetylide isomerization and addition of tris(dimethylamino) phosphine to the α-carbon atom of the bridging acetylide in $[Fe_2(CO)_6(\mu\text{-}PPh_2)(\mu\text{-}\eta^1\text{:}\eta^2\text{-}C{\equiv}CCH_3)]$ (**5**) (Scheme 2). The C(1a)−C(2a) bond length of 1.32(3) Å is close to that expected for a carbon−carbon double bond between sp^2-hybridized carbon atoms (1.337 Å). The P(1)−C(1a) bond distance of 1.93(2) Å is substantially longer than that in **3a** and significantly longer than expected for a compound with zwitterionic phosphorus−ylide character; that is, there appears to be a significant contribution from the $\mu\text{-}\eta^1$:

Table 2. Selected Bond Distances (Å) and Angles (deg) for Compounds 3a and 4a

Fe(1)−Fe(2)	2.5767(11)	Fe(1)−C(1)	1.997(10)
Fe(1)−C(2A)	2.069(15)	Fe(2)−C(1A)	2.34(2)
Fe(2)−C(1)	1.838(8)	C(2)−P(1)	1.734(8)
Fe(1)−P(2)	2.1886(15)	Fe(2)−P(2)	2.2048(14)
C(1A)−P(1)	1.93(2)	C(1)−C(2)	1.350(13)
C(1A)−C(2A)	1.32(3)	C(2)−C(3)	1.630(11)
C(2A)−C(3)	1.450(16)		
Fe(1)−P(2)−Fe(2)	71.82(5)	Fe(1)−C(1)−C(2)	126.4(7)
C(3)−C(2A)−Fe(1)	141.3(11)	C(2)−C(1)−Fe(2)	149.0(8)
Fe(1)−C(2A)−C(1A)	105.2(12)	C(1)−Fe(1)−P(2)	71.5(2)
C(2A)−C(1A)−Fe(2)	107.3(13)	C(1)−Fe(2)−P(2)	74.0(3)
P(1)−C(1A)−Fe(2)	129.3(10)	C(1)−C(2)−C(3)	118.5(7)
C(1A)−C(2A)−C(3)	112.2(14)	C(1)−C(2)−P(1)	121.8(4)
C(2A)−C(1A)−P(1)	122.1(14)	C(3)−C(2)−P(1)	120.1(6)
P(2)−Fe(2)−C(1A)	82.7(4)	C(2A)−Fe(1)−P(2)	88.7(4)

η^1-acetylene resonance structure **III** (Chart 2). However, the iron−carbon distances of 2.069(15) and 2.34(2) Å for Fe(1)−C(2a) and Fe(2)−C(1a), respectively, are distinctly different, which suggests there is also a contribution from the ylide−carbene structure **IV**. For comparison, the P−C bond distances of 1.723(3) and 1.74(1) Å in the triethyl phosphite adducts $[Fe_2(CO)_6(\mu\text{-}PPh_2)(\mu\text{-}\eta^1\text{:}\eta^1\text{-}(CH_3)C{=}C\{P(OEt)_3\})]$[16] and $[Fe_2(CO)_6(\mu\text{-}PPh_2)(\mu\text{-}$

Chart 2

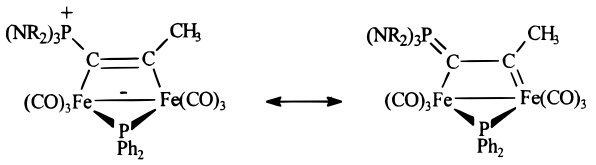

(III) **(IV)**

η^1:η^1-(Ph)C=C{P(OEt)$_3$})]^{24} are considerably shorter, even though the Fe−C bond lengths of 2.04(1) Å, for both compounds, are of comparable length to Fe(1)−C(2a). The dihedral angle of 6.9° between the planes containing P(1), C(1a), C(2a) and C(3), C(2a), C(1a) shows a small rotation about the C(1a)−C(2a) bond, which results in a puckering of the four-membered Fe_2C_2 ring structure.

Isomerization of [Fe$_2$(CO)$_6$(μ-PPh$_2$){μ-η^1:η^2-C(H)-C=C=CH$_2$}] (1). In an effort to understand the role of protonation in controlling the product distribution and regioselectivity of the reaction between **1** and P(NR$_2$)$_3$, the protonation of **1** was examined in detail. Protonation of a chloroform solution of **1** with HBF_4 led to a rapid and quantitative rearrangement (~10 min) to its σ−η-acetylide isomer [Fe$_2$(CO)$_6$(μ-PPh$_2$)(μ-η^1:η^2-C≡CCH$_3$)] (**5**), a transformation conveniently monitored by IR, ^{1}H, and ^{31}P spectroscopy. Treatment of a chloroform solution of **1** with HBF_4 affords a deep red solution with new absorption bands at 2093, 2059, 2032, and 2003 cm^{-1}, which are rapidly replaced by bands at 2071, 2032, 2002, and 1958 cm^{-1}, the latter corresponding to **5**. The high frequency of these former bands are within the range expected for protonation of the hydrocarbyl bridge and consistent with the formation of a cationic complex with reduced M−CO π-back-bonding.[23a] The low-temperature (−40 °C) ^{1}H NMR spectrum of a sample of **1** treated with HBF_4 showed the presence of a low-field doublet at δ 9.05 (J_{PH} = 46.1 Hz) and a high-field singlet at δ 1.60 (3H), which is consistent with the fragments Fe−C−H and Fe−C−CH$_3$, respectively. The absence of a high-field signal in the region δ 0 to −20 ppm confirmed that this intermediate was not a metal hydride. In the ^{31}P NMR spectrum a singlet at δ 42.0 is high-field shifted with respect to the phosphido bridge in **1** (δ 173.9). Such high-field shifts generally indicate a significant perturbation of the metal−metal interaction or P−C bond formation to give a tertiary phosphine derivative.[19] The deep red coloration associated with this intermediate persists for several hours at −40 °C but rapidly disappears upon warming to room temperature to give a deep orange solution of **5**, identified by ^{1}H, ^{13}C, and ^{31}P NMR spectroscopy and elemental analysis. These spectroscopic characteristics are consistent with the rearrangement of **1** into **5** via a short-lived spectroscopically observable intermediate. Interestingly, while addition of CF_3CO_2H to a chloroform solution of **1** at −40 °C also results in isomerization to give **5**, there was no observable intermediate, as evidenced by a persistent yellow coloration and the absence of a high-field signal in the ^{31}P NMR spectrum of the reaction mixture. Isotope labeling experiments using CF_3CO_2D and **1** gave a mixture of two isotopomers, [Fe$_2$(CO)$_6$(μ-PPh$_2$)(μ-η^1:η^2-C≡CCH$_3$)] (**5**-d_0) and [Fe$_2$(CO)$_6$(μ-PPh$_2$)(μ-η^1:η^2-C≡CCH$_2$D)] (**5**-d_1), identified in the ^{1}H{^{31}P} NMR spectrum as a singlet at δ 1.51 and a triplet ($^2J_{HD}$ = 2.4 Hz) at 14.6 ppb lower frequency (7.3 Hz at 500 MHz) due to the deuterium isotope shift of the methyl resonance. Notably, the ratio of **5**-d_0 to **5**-d_1 depends markedly on the amount of acid present, the concentration of **5**-d_1 increasing with increasing CF_3CO_2D.

On the basis of the ^{1}H and ^{31}P data described above and previous literature precedent (vide infra), one possible pathway for this isomerization involves regioselective protonation at C$_\gamma$ to afford **V** and insertion of the bridging propyne into an Fe−P bond of the phosphido group to give a five-electron donor diphenylphosphino-functionalized σ−η-alkenyl bridge **VI** (Scheme 3). At first site, regiospecific protonation at C$_\gamma$ would be expected to generate the thermodynamically favored cation **V**, which could be present as several constitutional isomers, **Va**−**c**, a cationic η^1:η^1-propyne-bridged structure **Va**, and the two carbocation−carbene structures **Vb** and **Vc**. Rather than lose H$^+$, **V** would then undergo P−C bond formation to generate the longer-lived spectroscopically observed intermediate [Fe$_2$(CO)$_6$-(μ-PPh$_2$)(μ-η^1(C):η^2(C):η^1(P)-{HC=CMe(PPh$_2$)})]$^+$ (**VI**), bridged by a diphenylphosphino-functionalized σ−η-alkenyl ligand. As noted earlier, the most compelling evidence for this intermediate is the upfield shift of the ^{31}P resonance and signals in the ^{1}H NMR spectrum (vide supra), although its precise structure is unclear. This intermediate is stable in solution below −40 °C but at higher temperatures readily converts into **5**. However, this pathway does not account for the deuterium labeling studies which gave **5**-d_1 and **5**-d_0 from the reaction between **1** and CF_3CO_2D. Direct protonation at C$_\gamma$ should give isotopomers with the same enrichment as the deuterium source, namely 99.5% CF_3CO_2D. Moreover, since the ratio of **5**-d_1 and **5**-d_0 depends on the concentration of CF_3CO_2D, **1** must react with H$^+$ to afford a kinetic regioisomeric cation which is in rapid equilibrium with uncomplexed acid. We have shown that **5** is stable toward H−D exchange at the methyl group since chloroform solutions of freshly prepared **5** and CF_3CO_2D do not incorporate deuterium even after stirring for 48 h at room temperature. Thus, alternative mechanisms must be considered to account for these observations (Scheme 4), the most likely of which involves initial protonation at C$_\alpha$ to give the allene-bridged cation [Fe$_2$(CO)$_6$(μ-PPh$_2$){μ-η^1:η^1-H$_2$C=C=CCH$_2$}]$^+$, **VIIa**−**c** (pathway a), or protonation at C$_\beta$ to generate the vinyl-carbene-bridged cation **VIIIa**−**c** (pathway b), followed by hydrogen migration to give **V**, the propyne-bridged cation common to Scheme 3. Clearly, whatever the mechanism of isomerization, the vinylidene and dimetallacyclobutene products isolated from the reaction between **1** and P(NMe$_2$)$_3$, in the presence of acid, result from nucleophilic addition to the α- and β-carbon atoms of the acetylide bridge in [Fe$_2$(CO)$_6$(μ-PPh$_2$){μ-η^1:η^2-C≡CCH$_3$}], and not from a nucleophilic addition hydrogen migration sequence. This has been confirmed by the independent synthesis of **5** and its reaction with P(NMe$_2$)$_3$, which was found to give a 67:33 mixture **3a** and **4a**, after purification by column chromatography and crystallization.

(24) Wong, Y. S.; Paik, H. N.; Chieh, P. C.; Carty, A. J. *J. Chem. Soc., Chem. Commun.* **1975**, 309.

Scheme 3

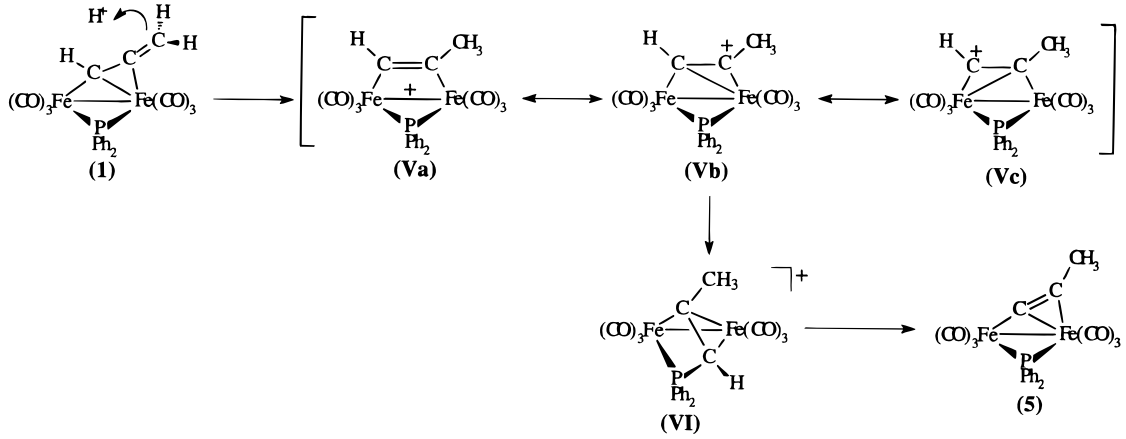

Scheme 4

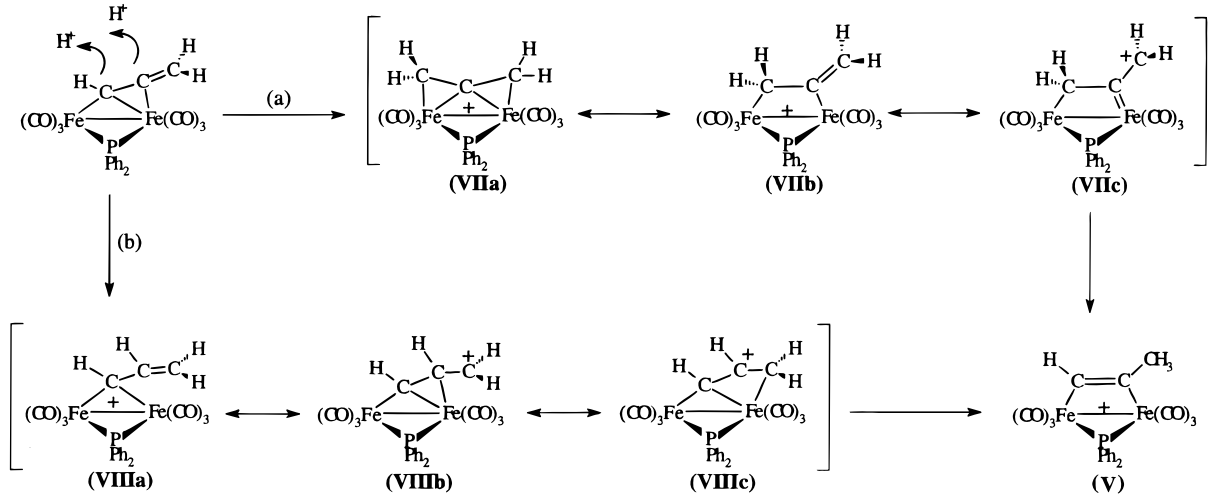

Mononuclear metal allenyl complexes have previously been reported to undergo allenyl to propynyl rearrangement via cationic η^2-propyne intermediates. Elegant studies by Gladysz and co-workers have shown that the η^2-allene cation $[(\eta^5\text{-}C_5H_5)Re(NO)(PPh_3)(\eta^2\text{-}H_2C{=}C{=}CH_2)]^+$ converts into the methyl acetylide $[(\eta^5\text{-}C_5H_5)Re(NO)(PPh_3)(\eta^1\text{-}C{\equiv}CCH_3)]$ via neutral η^2-allenyl and cationic η^2-propyne intermediates.[25] Similarly, the acid-promoted isomerization of $[(\eta^5\text{-}C_5H_5)Fe(CO)_2\{\eta^1\text{-}(H)C{=}C{=}CH_2\}]$ to $[(\eta^5\text{-}C_5H_5)Fe(CO)_2(\eta^1\text{-}C{\equiv}CCH_3)]$ involves protonation at the terminal $=CH_2$ substituent to give a cationic η^2-propyne intermediate.[26] Templeton and co-workers have also reported that deprotonation of [Tp′-$(CO)_2W(\eta^2\text{-}PhC{\equiv}CCH_3)$] [Tp′ = hydridotris(3,5-dimethylpyrazolyl)borate] produces a nucleophilic allenyl synthon that reacts with electrophiles to give η^2-alkyne derivatives.[27] If our neutral $\sigma-\eta$-allenyl complex were to react similarly, the intermediate would be a cationic propyne-bridged complex, stabilized by contributions from structures **Va**−**c**. However, it appears that **V** is the thermodynamic product of protonation, while either C_α or C_β is the kinetically preferred site for protonation.

Thermal Decarbonylation of $[Fe_2(CO)_6(\mu\text{-}PPh_2)(\mu\text{-}\eta^1{:}\eta^3\text{-}HC{=}C\{P(NR_2)_3\}CH_2)]$ (2a−c). Upon standing under an inert atmosphere, toluene solutions of **2a**−**c** smoothly decarbonylate over several days to afford the η^3-vinylcarbene complex $[Fe_2(CO)_5(\mu\text{-}PPh_2)(\mu\text{-}\eta^1{:}\eta^3\text{-}C(H)C\{P(NR_2)_3\}CH_2)]$ (R = Me, **6a**; R = Et, **6b**; R = ^{n}Pr, **6c**), a transformation that occurs more rapidly (1−2 h) in refluxing toluene (eq 1). In the $^{31}P\{^1H\}$ NMR spectrum

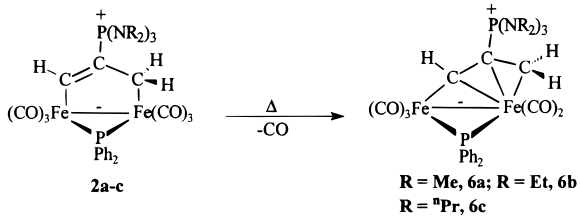

2a-c **R = Me, 6a; R = Et, 6b; R = ^{n}Pr, 6c** (1)

of **6a** two doublets at δ 145.7 and 56.5 have been assigned to the phosphido bridge and the carbon-bound tris(dimethylamino) phosphine, respectively. In the ^1H NMR spectrum of **6a** three distinct resonances at δ 5.25 (t, $^3J_{PH} = {}^3J_{PH} = 18$ Hz), 2.40 (d, $^3J_{PH} = 9.5$ Hz), and 2.02 (d, $^3J_{PH} = 21.7$ Hz) have been assigned to the protons attached to the bridging vinylcarbene. $^1H-{}^{13}C$ 2D-correlated NMR studies have shown that the low-field doublet belongs to the proton attached to the bridging carbene, while the two remaining signals are associated with the vinyl substituent, one of which shows a large trans vinylic coupling constant of $^3J_{PH} =$

(25) Pu, J.; Peng, T.-S.; Arif, A. M.; Gladysz, J. A. *Organometallics* **1992**, *11*, 3232.

(26) (a) Jolly, P. W.; Pettit. *J. Organomet. Chem.* **1968**, *12*, 491. (b) Ariyaratne, J. K. P.; Green, M. L. H. *J. Organomet. Chem.* **1963**, *1*, 90. (c) Johnson, M. D.; Mayle, C. *Chem. Commun.* **1969**, 192.

(27) (a) Gamble, A. S.; Birdwhistell, K. R.; Templeton, J. L. *J. Am. Chem. Soc.* **1990**, *112*, 1818. (b) Collins, M. A.; Feng, S. G.; White, P. A.; Templeton, J. L. *J. Am. Chem. Soc.* **1992**, *114*, 3771.

Scheme 5

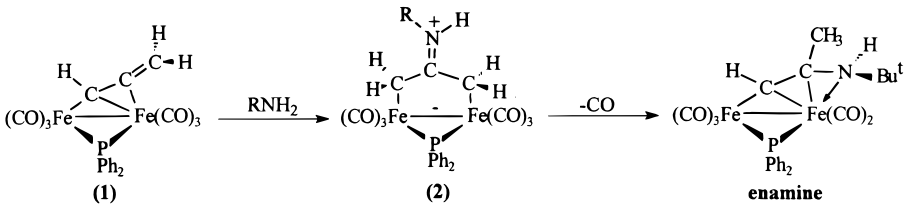

21.5 Hz and the other a smaller cis vinylic coupling of 9.4 Hz. In the ^{13}C NMR spectrum a low-field doublet at δ 190.2 ($^2J_{PC} = 18.1$ Hz) belongs to the bridging carbene carbon and appears in the same region as that previously reported for the vinyl carbene complexes $[Cp_2(CO)Fe_2(\mu\text{-}CO)\{\mu\text{-}\eta^1\text{:}\eta^3\text{-}(E)\text{-}CHC(CH_3)\text{=}CHCH_3\}]$,[28] $[Cp_2(CO)Fe_2(\mu\text{-}CO)\{\mu\text{-}\eta^1\text{:}\eta^3\text{-}(E)\text{-}C(CO_2Me)C(CO_2Me)\text{=}CHCH_3\}]$,[29] and $[Cp_2(CO)Ru_2(\mu\text{-}CO)\{\mu\text{-}\eta^1\text{:}\eta^3\text{-}(E)\text{-}CHC(R')\text{=}CH_2\}]$ (R′ = H, Me).[30] The central carbon atom of the bridging hydrocarbon appears at δ 136.9 (dd, $^1J_{PC} = 92.0$ Hz, $^3J_{PC} = 16.0$ Hz) and is strongly coupled to the tris(dialkylamino) phosphine phosphorus atom, which might possibly reflect ylide character in the P−C bond. The terminal vinylic carbon appears as a doublet of doublets at δ 17.1 ($^2J_{PC} = 14.0$ Hz, $^2J_{PC} = 5.7$ Hz), the high-field chemical shift and coupling to both phosphorus atoms indicating that the carbon−carbon double bond must be metal coordinated. Overall, the transformation of **2a** into **6a** involves loss of CO and η^2-coordination of the C−C double bond of the dimetallacyclopentene (eq 1). This transformation is not reversible since **6a** does not react with CO or trimethyl phosphite to regenerate the dimetallacyclopentane framework. For comparison, we have previously reported that the dimetallacyclopentane derivatives $[Fe_2(CO)_6(\mu\text{-}PPh_2)\{\mu\text{-}\eta^1\text{:}\eta^1\text{-}H_2CC(NHR)CH_2\}]$ readily lose CO to afford the β-substituted enamines $[Fe_2(CO)_5(\mu\text{-}PPh_2)\{\mu\text{-}\eta^1(C)\text{:}\eta^2(C)\text{:}\eta^1(N)\text{-}(H)C\text{=}CCH_3(NHR)\}]$, via 1,3-hydrogen migration and coordination of the amino functionality (Scheme 5).[10a]

As these are the first examples of diiron zwitterionic vinylcarbene-bridged complexes to be prepared, a single-crystal X-ray analysis of **6b** was undertaken, the result of which is shown in Figure 4, with selected bond lengths and angles listed in Table 3. The molecular structure clearly shows two iron atoms separated by a distance of 2.5981(3) Å and bridged asymmetrically by a phosphido ligand (Fe(1)−P(2) = 2.1752(5) Å; Fe(2)−P(2) = 2.2325(5) Å) and a three carbon atom bridging hydrocarbon, σ-bonded to Fe(2) (Fe(2)−C(1) = 2.0064(16) Å) and η^3-coordinated to Fe(1) (Fe(1)−C(1) = 2.0258(15) Å; Fe(1)−C(2) = 2.0447(15) Å; Fe(1)−C(3) = 2.1123(19) Å). We can envisage contributions from three possible resonance forms: a μ-carbene with an η^2-coordinated vinylic substituent **IXa**, an η^3-coordinated 1-metallaallyl structure **IXb**, and a dimetallacyclopentene ring Fe(1), Fe(2), C(1), C(2), C(3) in which the ethylenic bond C(1)−C(2) is η^2-bound to Fe(2) **IXc**, as shown in Chart 3. The structural data suggest that the actual bonding within the Fe_2C_3 framework lies somewhere between these three extremes.[29,30] For instance, the difference in Fe−C bond lengths to C(1) (ΔFe−C = 0.0194 Å) indicates a contribution from **IXb** and **IXc**, and not solely the vinylcarbene resonance structure **IXa**. The close similarity in the carbon−carbon bond lengths within the bridging hydrocarbon (C(1)−C(2) = 1.422(2) Å and C(2)−C(3) = 1.425(2) Å) and the trigonal geometry of C(1), C(2), and C(3) favor the η^3-allylic structure **IXb**, whereas the ^1H NMR spectroscopic data support the metallacyclopentene formulation **IXc**. Knox and coworkers have reported that dimethylacetylenedicarboxylate reacts with the alkylidene complex $[Fe_2(CO)_2(\mu\text{-}CO)(\mu\text{-}CHMe)(\eta^5\text{-}C_5H_5)_2]$ via alkyne−alkylidene coupling

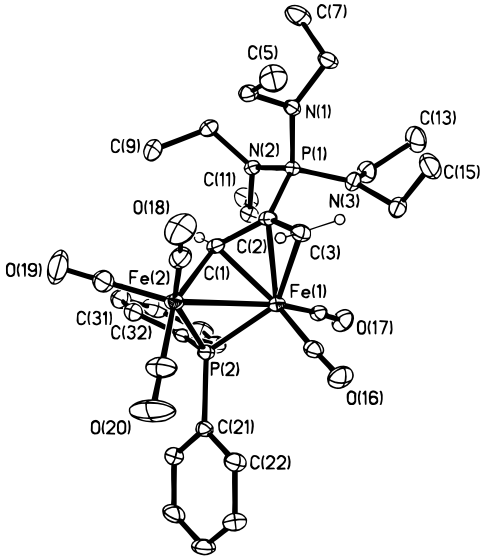

Figure 4. Molecular structure of $[Fe_2(CO)_5(\mu\text{-}PPh_2)(\mu\text{-}\eta^1\text{:}\eta^2\text{-}C(H)C\{P(NEt_2)_3\}CH_2)]$ (**6b**). Phenyl and NEt_2 hydrogen atoms have been omitted. Carbonyl carbons have the same numbers as oxygen atoms. Ellipsoids are at the 50% probability level.

Table 3. Selected Bond Distances (Å) and Angles (deg) for Compound 6b

Fe(1)−Fe(2)	2.5981(3)	Fe(1)−C(1)	2.0258(15)
Fe(2)−C(1)	2.0064(16)	Fe(1)−C(2)	2.0447(15)
Fe(1)−C(3)	2.1123(16)	Fe(1)−P(2)	2.1752(5)
Fe(2)−P(2)	2.2325(5)	C(1)−C(2)	1.422(2)
C(2)−C(3)	1.425(2)	C(2)−P(1)	1.8257(16)
Fe(1)−P(2)−Fe(2)	72.223(15)	C(3)−Fe(1)−P(2)	142.97(5)
C(2)−Fe(1)−P(2)	117.02(5)	C(1)−Fe(1)−P(2)	76.76(5)
C(1)−Fe(2)−P(2)	75.83(4)	C(2)−C(1)−Fe(2)	126.91(12)
C(2)− C(3)−Fe(1)	67.42(9)	P(1)−C(2)−Fe(1)	128.67(8)
C(1)−C(2)−C(3)	118.22(14)	C(1)−C(2)−P(1)	119.4(12)

(28) (a) Casey, C. P.; Woo, K. L.; Fagan, P. J.; Palermo, R. E.; Adams, B. R. *Organometallics* **1987**, *6*, 447. (b) Casey, C. P.; Meszaros, M. W.; Fagan, P. J.; Bly, R. K.; Marder, S. R.; Austin, E. A. *J. Am. Chem. Soc.* **1986**, *108*, 4043. (c) Casey, C. P.; Meszaros, M. W.; Fagan, P. J.; Bly, R. K.; Colborn, R. E. *J. Am. Chem. Soc.* **1986**, *108*, 4053.

(29) (a) Dyke, A. F.; Knox, S. A. R.; Naish, P. J. Taylor, G. E. *J. Chem. Soc., Chem. Commun.* **1980**, 203. (b) Dyke, A. F.; Guerchais, J. E.; Knox, S. A. R.; Roue, J.; Short, R. L.; Taylor, G. E. Woodward, P. *J. Chem. Soc. Chem. Commun.* **1981**, 537. (c) Dyke, A. F.; Knox, S. A. R.; Morris, M. J.; Naish, P. *J. Chem. Soc., Dalton Trans.* **1983**, 1417. (d) Dyke, A. F.; Knox, S. A. R.; Naish, P. J. Taylor, G. E. *J. Chem. Soc., Dalton Trans.* **1982**, 1297. (e) Gracey, B. P.; Knox, S. A. R.; Macpherson, K. A.; Orpen, A. G. Stobart, S. R. *J. Chem. Soc., Dalton Trans.* **1985**, 1935.

(30) Elsenstadt, A.; Efraty, A. *Organometallics* **1982**, *1*, 1101.

Chart 3

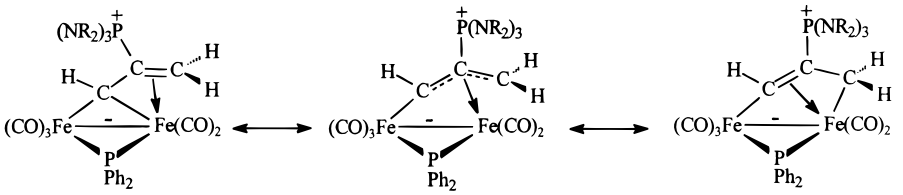

(IXa) **(IXb)** **(IXc)**

to give the vinylcarbene derivative $[(\eta^5\text{-}C_5H_5)_2(CO)Fe_2(\mu\text{-}CO)\{\mu\text{-}C(CO_2Me)C(CO_2Me)CHR^1\}]$.[29] In this case the bridging carbon is equidistant from both iron atoms with the vinyl fragment symmetrically bonded to one iron. The P(1)−C(2) bond length of 1.8257(16) Å is much longer than that in **2a** and close to a P−C single bond, confirming that **6b** is zwitterionic with little phosphorus ylide character, perhaps not surprising considering the multiple bond character in the carbon framework of the C_3 bridge.

While the thermal decarbonylation of **2a** gives **6a** as the sole product in near quantitative yields, under the same conditions of thermolysis **2b** gave **6b** together with a second slower moving product, identified in the first instance by single-crystal X-ray crystallography as $[Fe_2(CO)_5(\mu\text{-}PPh_2)\{\mu\text{-}\eta^1\text{:}\eta^2\text{-}P(NEt_2)_3C(O)CHC{=}CH_2\}]$ (**7b**), an isomer of **2b**, subsequently characterized by ^1H and ^{13}C NMR spectroscopy and elemental analysis (eq 2).

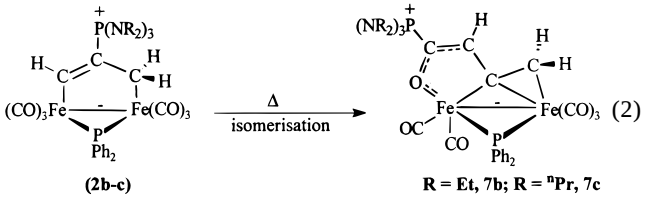

(2b-c) **R = Et, 7b; R = ^{n}Pr, 7c** (2)

In the ^1H NMR spectrum the two protons attached to the β-vinyl carbon appear as distinct doublets at δ 3.55 ($^3J_{PH}$ = 11.3 Hz) and δ 1.69 ($^3J_{PH}$ = 8.0 Hz), while the unique proton adjacent to the carbonyl carbon, C(O)-C*H*C=CH$_2$, gives rise to a broad singlet at δ 6.70. In the $^{13}C\{^1H\}$ NMR spectrum the α-vinyl carbon appears as a doublet at δ 167.2, which is in the region expected for a $\sigma-\eta$-coordinated alkenyl ligand[31] and the carbonyl carbon of the bridging hydrocarbyl ligand as a doublet at δ 160.6, with an exceptionally large phosphorus−carbon coupling constant ($^1J_{PC}$ = 159.1 Hz). The two remaining signals associated with the hydrocarbyl bridge, the CH carbon α to the ketonic carbonyl and the β-vinyl carbon, appear as doublets at δ 133.6 ($^3J_{PC}$ = 8.8 Hz) and 54.8 ($^2J_{PC}$ = 6.5 Hz), respectively. In the carbonyl region, three separate resonances, two doublets at δ 219.3 and 215.2 associated with the Fe(CO)$_2$ fragment and one broad singlet at δ 216.6 corresponding to the three carbonyls of the Fe(CO)$_3$ fragment, reveal that $\sigma-\eta$-vinyl fluxionality is slow at room temperature.[32] Since the carbonyl group attached to the α-carbon atom of **7b** forms a five-membered chelate, the μ-alkenyl ligand is unlikely to undergo $\sigma-\eta$-site exchange via the "windshield wiper" mechanism because such a process would involve cleavage of the anchoring metal−carbonyl interaction and internuclear migration of a carbonyl ligand.

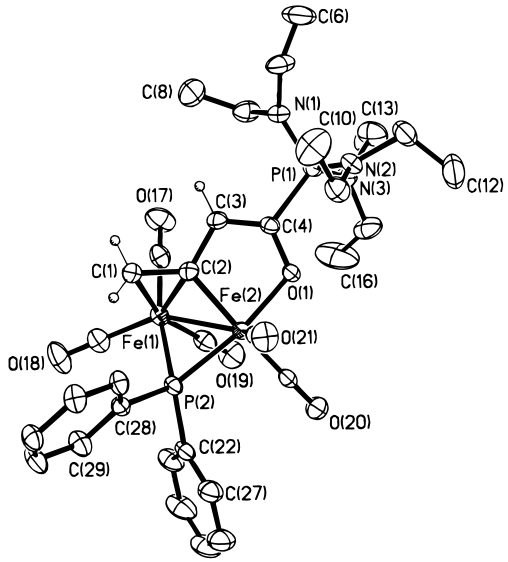

Figure 5. Molecular structure of $[Fe_2(CO)_5(\mu\text{-}PPh_2)\{\mu\text{-}\eta^1\text{:}\eta^2\text{-}\{P(NEt_2)_3\}C(O)CHC{=}CH_2\}]$ (**7b**). Phenyl and N*Et*$_2$ hydrogen atoms have been omitted. Carbonyl carbons have the same numbers as oxygen atoms. Ellipsoids are at the 50% probability level.

A single-crystal X-ray study on **7b** was undertaken to provide precise details on the nature of the bridging hydrocarbyl ligand and its mode of coordination to the diiron fragment. A perspective view of the molecular structure is shown in Figure 5, and a selection of bond lengths and angles is listed in Table 4. The molecular structure identifies **7b** as $[Fe_2(CO)_5(\mu\text{-}PPh_2)\{\mu\text{-}\eta^1\text{:}\eta^2\text{-}P(NEt_2)_3C(O)CHC{=}CH_2\}]$, for which the principle feature of interest is the unusual α-CHC(O)P(NMe$_2$)$_3$-functionalized $\mu-\sigma-\eta^2$-alkenyl ligand, σ-bonded to Fe(2) (Fe(2)−C(2) = 1.959(2) Å) and η^2-bonded to Fe(1) (Fe(1)−C(1) = 2.143(2) Å; Fe(1)−C(2) = 2.171(2) Å). Overall the isomerization of **2b** into **7b** involves P(NEt$_2$)$_3$−CO-allenyl coupling (eq 2), the precise details of which will be discussed in the following section. Atoms Fe(2), O(1), C(4), C(3), and C(2) form a five-membered planar metallacycle, the largest deviation from the mean plane of the ring system being 0.0426 Å. The bond length pattern within this ring is consistent with delocalization of the bonding electron density over

(31) (a) MacLaughlin, S. A.; Doherty, S. Taylor, N. J.; Carty, A. J. *Organometallics* **1992**, *11*, 4315. (b) Hogarth, G.; Lavender, M. H. *J. Chem. Soc., Dalton Trans.* **1994**, 3389.

(32) (a) Xue, Z.; Sieber, W. J.; Knobler, C. B.; Kaesz, H. D. *J. Am. Chem. Soc.* **1990**, *112*, 1825. (b) Shapley, J. R. Richter, S. I.; Tachikawa, M.; Keister, J. B. *J. Organomet. Chem.* **1975**, *94*, C43. (c) Farrugia, L.; Chi, Y.; Tu, W.-C. *Organometallics* **1993**, *12*, 1616. (d) Casey, C. P.; Marder, S. R.; Adams, B. R. *J. Am. Chem. Soc.* **1985**, *107*, 7700, and references therein.

Table 4. Selected Bond Distances (Å) and Angles (deg) for Compounds 7b

Fe(1)−Fe(2)	2.6598(7)	Fe(1)−P(2)	2.2541(8)
Fe(2)−P(2)	2.1631(7)	Fe(2)−O(1)	1.9807(14)
Fe(1)−C(1)	2.143(2)	Fe(1)−C(2)	2.171(2)
Fe(2)−C(2)	1.959(2)	C(1)−C(2)	1.406(3)
C(2)−C(3)	1.456(3)	C(3)−C(4)	1.353(3)
C(4)−O(1)	1.310(2)	C(4)−P(1)	1.803(2)
Fe(1)−P(2)−Fe(2)	74.01(2)	O(1)−Fe(2)−P(2)	157.38(5)
C(1)−Fe(1)−P(2)	85.91(7)	C(2)−Fe(1)−P(2)	81.05(6)
C(1)−C(2)−Fe(2)	129.46(1)	C(3)−C(2)−Fe(2)	109.52(15)
C(2)−C(1)−Fe(1)	72.05(13)	C(3)−C(2)−Fe(1)	120.57(14)
Fe(1)−C(2)−C(1)	69.91(13)	C(1)−C(2)−C(3)	120.6(2)
C(4)−C(3)−C(2)	114.70(19)	O(1)−C(4)−C(3)	120.06(18)
C(4)−O(1)−Fe(2)	111.72(13)	C(3)−C(4)−P(1)	122.39(16)
O(1)−C(4)−P(1)	117.28(5)		

Fe(2), O(1), C(4), and C(3), as is the planar nature of C(2), C(3), and C(4). For instance, the carbon oxygen bond length of 1.310(2) Å for C(4)−O(1) is considerably longer than the equivalent carbon−oxygen double bond length of 1.229(3) Å (Δ = 0.081 Å) in the ester-coordinated carbonyl complex $[Fe_2(CO)_5(\mu\text{-}PPh_2)(\mu\text{-}\eta^1\text{:}\eta^2\text{-}\{^i PrOC(O)CH_2\}C{=}CH_2)]$ (**10**) (vide infra),[11] whereas the carbon−carbon bond length of 1.353(3) Å for C(4)−C(3) is substantially shorter than expected for a single bond (~1.50 Å).[33] The sum of the angles at C(4) (359.73°) and C(2) (359.68°) is consistent with sp^2 hybridization. The structure of **7b** is closely similar to the β,γ-unsaturated carbonyl compounds $[Fe_2(CO)_5(\mu\text{-}PPh_2)(\mu\text{-}\eta^1\text{:}\eta^2\text{-}\{NuC(O)CH_2\}C{=}CH_2)]$ (Nu = OR, NHR, alkyl).[9,10b,11] The most notable difference between **7b** and these β,γ-unsaturated carbonyl-bridged dimers is the five-membered metallacycle, which in $[Fe_2(CO)_5(\mu\text{-}PPh_2)(\mu\text{-}\eta^1\text{:}\eta^2\text{-}\{NuC(O)CH_2\}C{=}CH_2)]$ is best described in terms of a saturated FeC_3O chelate ring formed by coordination of the ester carbonyl, whereas the C−C and C−O bond length pattern in **7b** indicates significant delocalization within the metallacycle. The bonding within the metallacycles of **7a**−**c** and **10** is also supported by the values of ν(CO) for the bridging hydrocarbyl ligands. Those for **7a**−**c** are low-frequency shifted and appear between 1583 and 1587 cm^{-1}, whereas that for **10** appears at 1635 cm^{-1}. On the basis of the structural and spectroscopic data the bonding in **7a**−**c** is clearly delocalized, while that in **10** is most aptly described as a localized five-membered metallacycle by virtue of coordination of the ester carbonyl. A comparison of the structure of **7b** with $[Fe_2(CO)_5(\mu\text{-}PPh_2)(\mu\text{-}\eta^1\text{:}\eta^2\text{-}\{^i PrOC(O)CH_2\}C{=}CH_2)]$ (**10**),[11] shown in Figure 6, illustrates the similarity in the connectivity of the bridging hydrocarbyl fragments and the differences between the bonding within their metallacyclic frameworks. The P(1)−C(4) bond length of 1.803(2) Å is substantially longer than expected for a phosphorus−carbon ylide bond,[34] which is probably a result of the delocalization of electron density over the five-membered ring. For comparison, the P(1)−C(4) distance in **7b** is considerably longer than the P−CH_2 distance of 1.702(2) Å in $[(PPhCH_2)_2NLiCH_2PPh_3]_n$, a lithium complex of a neutral P^V ylide.[35] Moreover, P(1) is close to tetrahedral, with most of its angles near the ideal tetrahedral angle, and the P(1)−C(4) bond distance is consistent with that of a four-coordinate phosphonium salt.[36] On the basis of these data, the hydrocarbyl bridge in **7b** may be described as a α-phosphonium-alkoxide-functionalized σ−η-alkenyl ligand[37] with the phosphonium cation attached to the carbonyl carbon and the coordinated alkoxide anion forming the metallacycle. The C(1)−C(2) bond length of 1.406(3) Å is intermediate between a double and single bond, and in this regard, **7b** closely resembles other diiron alkenyl complexes.[38] The σ−η-alkenyl fragment in **7b** adopts the familiar *exo* conformation; that is, the α-carbon of the alkenyl ligand is orientated away from the phosphido bridge, presumably to avoid unfavorable steric interactions between the substituent on C_α and the phenyl rings of the bridging PPh_2 ligand.[31] The two iron atoms are asymmetrically bridged by the phosphido ligand (Fe(1)−P(2) = 2.2541(8) Å; Fe(2)−P(2) = 2.1631(7) Å) and one of the iron atoms Fe(1) carriers three carbonyl ligands while the other Fe(2) carries two.

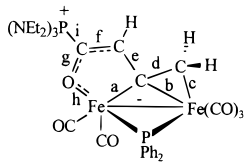

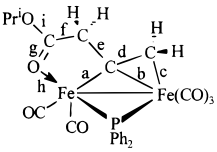

Bond type	bond distance (Å) for **7b**	bond distance (Å) for **10**
a	1.959(2)	1.956(3)
b	2.171(2)	2.135(3)
c	2.143(2)	2.179(3)
d	1.406(3)	1.398(4)
e	1.456(3)	1.505(4)
f	1.353(3)	1.482(4)
g	1.310(2)	1.229(3)
h	1.9807(14)	2.074(2)
i	1.803(2)	1.314(3)

Figure 6. Comparison of Fe−C, C−C and C−O bond lengths in $[Fe_2(CO)_5(\mu\text{-}PPh_2)\{\mu\text{-}\eta^1\text{:}\eta^2\text{-}\{P(NEt_2)_3\}C(O)CHC{=}CH_2\}]$ (**7b**) and $[Fe_2(CO)_5(\mu\text{-}PPh_2)\{\mu\text{-}\eta^1\text{:}\eta^2\text{-}\{^i PrOC(O)CH_2C{=}CH_2\}]$ (**10**).

Isomerization of $[Fe_2(CO)_5(\mu\text{-}PPh_2)$ $(\mu\text{-}\eta^1\text{:}\eta^2\text{-}C(H)C\text{-}\{P(NR_2)_3\}CH_2)]$ to $[Fe_2(CO)_5(\mu\text{-}PPh_2)$ $\{\mu\text{-}\eta^1\text{:}\eta^2\text{-}\{P(NR_2)_3C(O)CHC{=}CH_2\}]$. The isomerization of **2b**,**c** into **7b**,**c** is intriguing since the latter closely resembles the β,γ-unsaturated esters (Nu = OR), amides (Nu = NRH), and ketones (Nu = R) $[Fe_2(CO)_5(\mu\text{-}PPh_2)(\mu\text{-}\eta^1\text{:}\eta^2\text{-}\{NuC(O)CH_2\}C{=}CH_2)]$ isolated from the reaction between **1** and the corresponding alcohol, amine, and

(33) *Molecular Structures and Dimensions*; Kennard, O., Watson, D. G., Allen, F. H., Isaacs, N. W., Motherwell, W. D. S., Petterson, R. C., Town, W. G., Eds.; N. V. A. Oosthoek: Utrecht, 1969; Vol. A1, p 52.

(34) Carroll, P. J.; Titus, D. D. *J. Chem. Soc., Dalton Trans.* **1977**, 134. (b) Burzlaff, H.; Wilheim, E.; Bestmann, H. J. *Chem. Ber.* **1977**, *110*, 3368.

(35) Armstrong, D. R.; Davidson, M. G.; Moncrieff, D. *Angew. Chem., Int. Ed. Engl.* **1995**, *34*, 478.

(36) Carmona, E.; Gutierrez-Puebla, E.; Monge, A.; Perez, P. J. S. Slachez, L. *Inorg. Chem.* **1989**, *28*, 2120.

(37) (a) Tikkannen, W.; Kim, A. L.; Lam, K. B.; Ruekert, K. *Organometallics* **1995**, *14*, 1525. (b) Tikkanen, W.; Ziller, W. *Organometallics* **1991**, *10*, 2266.

(38) (a) Hogarth, G.; Lavender, M. H.; Shukri, K. *Organometallics* **1995**, *14*, 2325. (b) Orpen, A. G. *J. Chem. Soc., Dalton Trans.* **1983**, 1427. (c) Hogarth, G.; Lavender, M. H. *J. Chem. Soc., Dalton Trans.* **1992**, 2759. (d) Boothman, J.; Hogarth, G. *J. Organomet. Chem.* **1992**, *437*, 201. (e) Hogarth, G.; Lavender, M. H. Shukri, K. *J. Organomet. Chem.* **1997**, *527*, 247.

Scheme 6

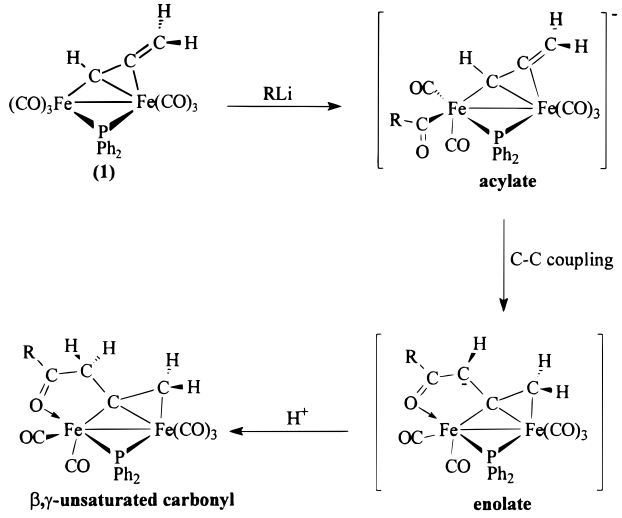

alkyllithium reagent, respectively (eq 3).[9−11] One pos-

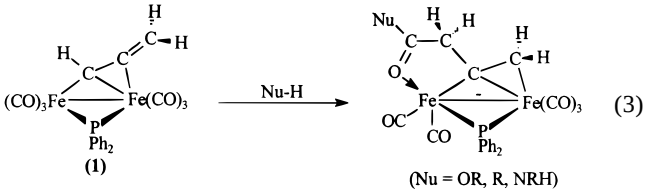

(3)

sible mechanism for the conversion of **1** into the β,γ-unsaturated ketones was suggested to involve nucleophilic attack of R^- at CO, to give an acylate intermediate, migration of the RCO group to C_α of the allenyl, followed by protonation (Scheme 6). Given the structural similarity between **7b** and these β,γ-unsaturated carbonyl derivatives, it is tempting to suggest that **7b** forms via a similar pathway, i.e. nucleophilic attack of $P(NEt_2)_3$ at CO, to give a zwitterionic acylate intermediate followed by acyl−allenyl coupling.

While the dimetallacyclopentenes **2b**,**c** are thermodynamically unstable with respect to isomerization to **7b**,**c** (eq 2), albeit in competition with loss of carbon monoxide to give the vinyl carbene $[Fe_2(CO)_5(\mu\text{-}PPh_2)(\mu\text{-}\eta^3\text{-}C(H)C\{P(NR_2)_3\}CH_2)]$ (eq 1), their dimetallacyclopentane counterparts $[Fe_2(CO)_6(\mu\text{-}PPh_2)(\mu\text{-}\eta^1\text{:}\eta^1\text{-}H_2CC(NHR)CH_2]$ are considerably more stable and at elevated temperatures decarbonylation is the dominant reaction.[10a] In this regard, we have recently shown that $[Fe_2(CO)_6(\mu\text{-}PPh_2)(\mu\text{-}\eta^1\text{:}\eta^1\text{-}H_2CC\{NHR\}CH_2]$ does not isomerize to the β,γ-unsaturated amide $[Fe_2(CO)_5(\mu\text{-}PPh_2)(\mu\text{-}\eta^1\text{:}\eta^2\text{-}\{NHRC(O)CH_2\}C{=}CH_2)]$, but readily loses carbon monoxide to give the β-substituted enamine $[Fe_2(CO)_5(\mu\text{-}PPh_2)\{\mu\text{-}\eta^1\text{:}\eta^1\text{:}\eta^2\text{-}(H)C{=}CCH_3(NHR)\}]$, via 1,3-hydrogen migration and coordination of the amino group (Scheme 5).[10a] Both isomers $[Fe_2(CO)_6(\mu\text{-}PPh_2)(\mu\text{-}\eta^1\text{:}\eta^1\text{-}H_2CC\{NH^tBu\}CH_2)]$ and $[Fe_2(CO)_5(\mu\text{-}PPh_2)(\mu\text{-}\eta^1\text{:}\eta^2\text{-}\{NH^tBuC(O)CH_2\}C{=}CH_2)]$ have been isolated from the reaction between **1** and *tert*-butylamine, and in order to show that the former does not isomerize to the latter, a sample of $[Fe_2(CO)_6(\mu\text{-}PPh_2)\{\mu\text{-}\eta^1\text{:}\eta^1\text{-}H_2CC(NH^tBu)CH_2\}]$ was dissolved in diethyl ether and stirred at room temperature, conditions under which the rearrangement was expected to occur. We found no evidence for isomerization of $[Fe_2(CO)_6(\mu\text{-}PPh_2)(\mu\text{-}\eta^1\text{:}\eta^1\text{-}H_2CC\{NH^tBu\}CH_2)]$, even after 48 h, which indicates that these two products must form via different pathways, i.e. competing $P-C_\beta$ bond formation and amine−carbonyl−allenyl coupling, respectively. As expected in the absence of isomerization, thermolysis of a thf solution of $[Fe_2(CO)_6(\mu\text{-}PPh_2)\{\mu\text{-}\eta^1\text{:}\eta^1\text{-}H_2CC(NH^tBu)CH_2\}]$ results in clean quantitative transformation to the enamine-bridged product $[Fe_2(CO)_5(\mu\text{-}PPh_2)\{\mu\text{-}\eta^1(C)\text{:}\eta^2(C)\text{:}\eta^1(N)\text{-}(H)C{=}CCH_3(NH^tBu)\}]$, complete conversion requiring 2 h. Since $[Fe_2(CO)_6(\mu\text{-}PPh_2)\{\mu\text{-}\eta^1\text{:}\eta^1\text{-}H_2CC(NH^tBu)CH_2\}]$ and $[Fe_2(CO)_5(\mu\text{-}PPh_2)(\mu\text{-}\eta^1\text{:}\eta^2\text{-}\{NH^tBuC(O)CH_2\}C{=}CH_2)]$ do not interconvert, we are left to explain why the isomerization of $[Fe_2(CO)_6(\mu\text{-}PPh_2)(\mu\text{-}\eta^1\text{:}\eta^2\text{-}HC{=}C\{P(NR_2)_3\}CH_2)]$ (**2b**,**c**) to $[Fe_2(CO)_5(\mu\text{-}PPh_2)\{\mu\text{-}\eta^1\text{:}\eta^2\text{-}\{P(NR_2)_3C(O)CHC{=}CH_2\}]$ (**7b**,**c**) occurs under such mild conditions. At this stage the most plausible explanation, by analogy with the competitive formation of $[Fe_2(CO)_6(\mu\text{-}PPh_2)\{\mu\text{-}\eta^1\text{:}\eta^1\text{-}H_2CC(NHR)CH_2\}]$ and $[Fe_2(CO)_5(\mu\text{-}PPh_2)(\mu\text{-}\eta^1\text{:}\eta^2\text{-}\{NHRC(O)CH_2\}C{=}CH_2)]$ from the reaction between **1** and various amines, involves dissociation of phosphine from the kinetic regioisomeric intermediate **2b**,**c** to regenerate **1**, followed by phosphine−carbonyl−allenyl coupling to give the thermodynamically favored zwitterionic $\sigma\text{-}\eta^2$-alkenyl derivative **7b**,**c** (Scheme 7). A detailed study of the reaction between **1** and PPh_3 provides support in favor of this pathway.

Scheme 7

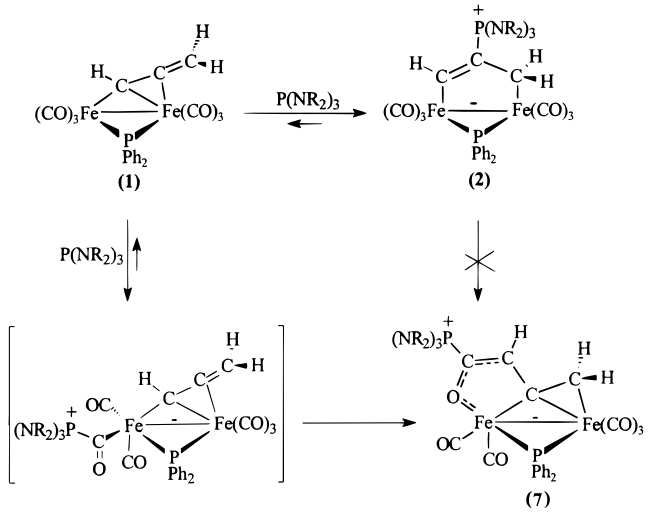

Preparation of $[Fe_2(CO)_6(\mu\text{-}PPh_2)(\mu\text{-}\eta^1\text{:}\eta^1\text{-}HC{=}C\{PPh_3\}CH_2)]$ (8) and Isomerization to $[Fe_2(CO)_5(\mu\text{-}PPh_2)\{\mu\text{-}\eta^1\text{:}\eta^2\text{-}PPh_3C(O)CH_2C{=}CH_2\}]$ (9). During the attempted isomerization of **1** to $[Fe_2(CO)_6(\mu\text{-}PPh_2)(\mu\text{-}\eta^1\text{:}\eta^2\text{-}C{\equiv}CCH_3)]$, the addition of triphenyl phosphine to a diethyl ether solution of **1** was found to give $[Fe_2(CO)_6(\mu\text{-}PPh_2)(\mu\text{-}\eta^1\text{:}\eta^1\text{-}HC{=}C\{PPh_3\}CH_2)]$ (**8**) in near quantitative yields. The reaction is conveniently monitored by TLC, which shows the gradual appearance of a single yellow slow moving band, the identity of which was confirmed by IR, ^1H, and ^{13}C NMR spectroscopy. The three protons attached to the hydrocarbyl bridge give rise to complex multiplets in the ^1H NMR spectrum, a characteristically low-field doublet at δ 7.90 ($^3J_{PH} = 27.2$ Hz), belonging to the methine proton, and a two-proton multiplet for the methylene protons at δ 1.12. In addition to the expected doublets at δ 207.8 and 7.8 ($^4J_{PP} = 10.1$ Hz) the ^{31}P NMR spectrum of **8** contains two

Scheme 8

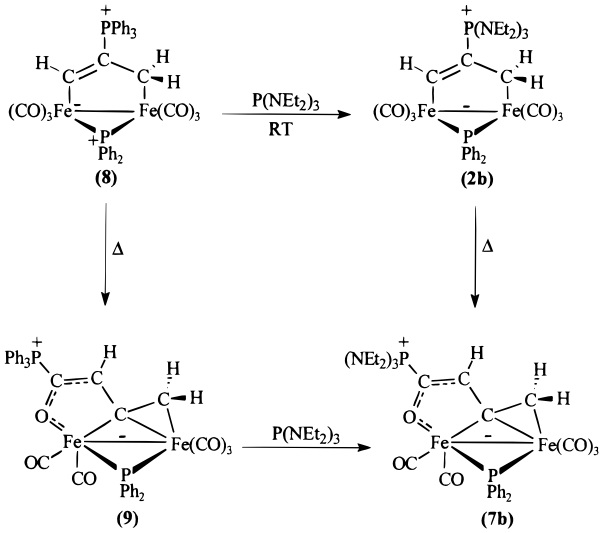

additional resonances at δ 173.9 and −4.9, even after several recrystallizations. These latter signals correspond to **1** and PPh_3, respectively, our first indication that dimetallacyclopentene derivatives exist in equilibrium with **1** and uncomplexed phosphine. We are confident that these signals are not the result of contamination since **1** clearly separates from **8** by column chromatography and is further purified by repeated crystallization. Variable-temperature ^{31}P NMR studies and phosphine exchange reactions provide additional support for this equilibrium. At room temperature the equilibrium ratio of **8** and **1** is 10:1, whereas upon cooling to −70 °C this changes to 3.5:1. In addition, thermolysis of a toluene solution of **8** with excess $P(NEt_2)_3$ results in exclusive formation of **7b**, whereas at room temperature phosphine substitution gives **2b**, as the sole product after chromatographic workup and crystallization (Scheme 8). We have also examined the behavior of **8** in the presence of tris(*p*-tolyl)phosphine to determine whether its isomerization to **9** is intra- or intermolecular (vide infra). Excess tris(p-tolyl)phosphine was added to a chloroform solution of **8** at room temperature. Examination of the ^{31}P NMR spectrum showed the disappearance of **8** and formation of a new compound presumed to be $[Fe_2(CO)_5(\mu\text{-}PPh_2)(\mu\text{-}\eta^1{:}\eta^1\text{-}HC{=}C\{(p\text{-tolyl})_3P\}CH_2)]$ (eq 4). Clearly, loss of PPh_3 is

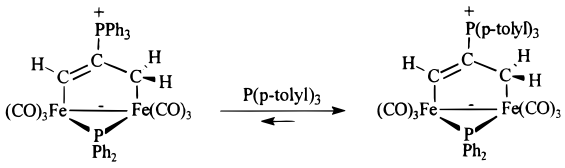

(4)

rapid and reversible at room temperature, suggesting that the isomerization of **8** to **9** is dissociative and further reinforcing the reaction mechanism outlined in Scheme 7.

Even though these spectroscopic characteristics are fully consistent with a dimetallacyclopentene formulation, the vastly disparate rates of isomerization of **8** and **2b** prompted us to investigate the solid-state structure of the former for a comparison. The molecular structure is shown in Figure 7, and a selection of relevant bond lengths and angles is given in Table 5. The solid-state

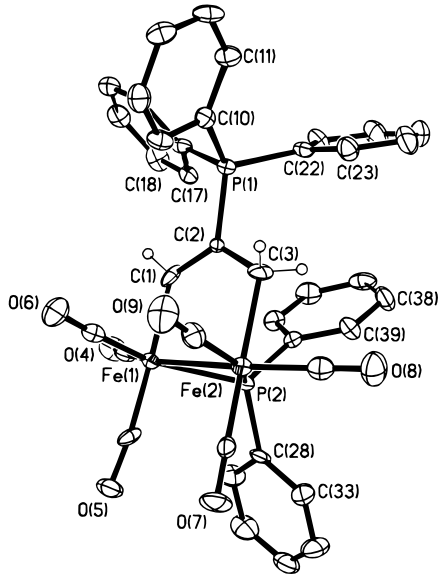

Figure 7. Molecular structure of $[Fe_2(CO)_6(\mu\text{-}PPh_2)(\mu\text{-}\eta^1{:}\eta^1\text{-}HC{=}C\{PPh_3\}CH_2)]$ (**8**). Phenyl hydrogen atoms have been omitted. Carbonyl carbons have the same numbers as oxygen atoms. Ellipsoids are at the 50% probability level.

Table 5. Selected Bond Distances (Å) and Angles (deg) for Compound 8

Fe(1)−Fe(2)	2.7382(19)	Fe(1)−P(2)	2.198(3)
Fe(2)−P(2)	2.188(3)	Fe(1)−C(1)	1.965(11)
Fe(2)−C(3)	2.110(10)	C(1)−C(2)	1.368(13)
C(2)−C(3)	1.490(13)	C(2)−P(1)	1.785(9)
C(3)−Fe(2)−P(2)	88.2(3)	C(1)−Fe(1)−P(2)	89.2(3)
C(2)−C(3)−Fe(2)	114.5(6)	C(2)−C(1)−Fe(1)	126.5(7)
C(1)−C(2)−P(1)	119.1(7)	C(3)−C(2)−P(1)	116.0(6)
C(1)−C(2)−C(3)	124.8(8)	Fe(1)−P(2)−Fe(2)	77.26(9)

structure of **8** is qualitatively identical to that of **2b** in that it consists of a dimetallacyclopentene ring with the C_3 hydrocarbyl bridge σ-bonded to Fe(1) (Fe(1)−C(1) = 1.965(11) Å) and Fe(2) (Fe(2)−C(3) = 2.110(10) Å). These bond lengths differ from the equivalent Fe−C bond lengths in **2a** in that the Fe−C(sp) bond, Fe(1)−C(1), is substantially shorter than that in **2b** (ΔFe−C = 0.077 Å), while the Fe−C(sp^2) bond, Fe(2)−C(3), is markedly longer (ΔFe−C = 0.050 Å). Overall, the Fe−C(sp) and Fe−C(sp^2) bonds in **2a** are of similar length (ΔFe−C = 0.018 Å), while the difference between Fe(1)−C(1) and Fe(2)−C(2) in **8** is significantly larger (ΔFe−C = 0.145 Å). The carbon−carbon bond lengths of 1.368(13) and 1.490(13) Å for C(1)−C(2) and C(2)−C(3), respectively, are similar to those in **2a**, as is the P(1)−C(2) bond length of 1.785(9) Å. The similarity in the P−C bond lengths in **2a** and **8** is somewhat surprising since the short Fe(1)−C(1) bond is suggestive of a greater contribution from the carbene−ylide resonance form in **8** compared with **2a**, which should be accompanied by increased P−C multiple bond character.[18] The remaining structural features associated with the metal atom framework and supporting ligands are similar to those of **2a**.

After standing for short periods of time solutions of **8** gradually darken, changing from deep yellow to orange-red, with TLC analysis revealing the appearance of a second slower moving orange band. This transformation is quantitative and complete within 2 h and considerably more rapid than the corresponding transformation

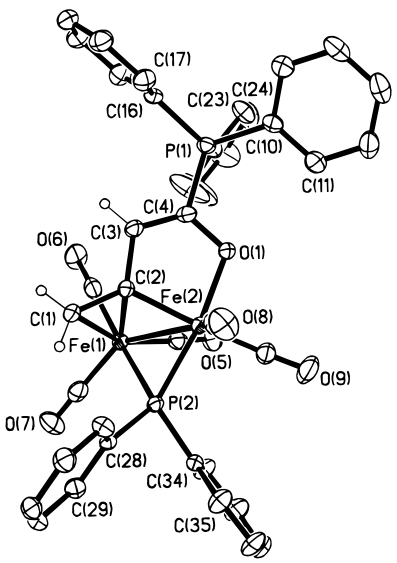

Figure 8. Molecular structure of $[Fe_2(CO)_5(\mu\text{-}PPh_2)\{\mu\text{-}\eta^1\text{:}\eta^2\text{-}PPh_3C(O)CH_2C{=}CH_2\}]$ (**9**). Phenyl atoms have been omitted. Carbonyl carbons have the same numbers as oxygen atoms. Ellipsoids are at the 50% probability level.

of **2b**,**c**. Purification of the product by column chromatography followed by crystallization from petroleum ether gave red crystals of $[Fe_2(CO)_5(\mu\text{-}PPh_2)\{\mu\text{-}\eta^1\text{:}\eta^2\text{-}PPh_3C(O)CHC{=}CH_2\}]$ (**9**), identified in the first instance by ^1H, ^{31}P, and IR spectroscopy and latter by single-crystal X-ray crystallography. In the ^1H NMR spectrum of **9** the two vinylic protons appear as complex multiples at δ 3.44 ($^3J_{PH}$ = 11.2 Hz, $^4J_{HH}$ = 2.1 Hz) and 1.69 ($^3J_{PH}$ = 8.0 Hz), while the remaining proton of the hydrocarbyl bridge gives rise to a low-field multiplet at δ 6.40 ($^3J_{PH}$ = 3.3 Hz, $^4J_{HH}$ = 2.1 Hz). This latter assignment was based on a comparison to the chemical shift of the corresponding proton in **7b**,**c**, identified using DEPT and $^{13}C-^1H$ correlated NMR experiments. In the $^{13}C\{^1H\}$ NMR spectrum of **9**, a doublet at δ 164.5 is assigned to the α-vinyl carbon, a doublet at 153.2, with a large phosphorus−carbon coupling constant ($^1J_{PC}$ = 93.1 Hz) to the $PPh_3C(O)$ carbonyl carbon, a doublet at δ 133.6 to the carbon adjacent to $PPh_3C(O)$, and a doublet at δ 56.2 to the β-vinyl carbon. Although the ^{31}P NMR spectrum of **9** contains two doublets at δ 162.7 and 1.6 ($^5J_{PP}$ = 5.5 Hz), which correspond to the bridging phosphido ligand and carbon-bound triphenyl phosphine, respectively, upon standing an equilibrium mixture of **9** and **1** formed, as evidenced by the appearance of additional resonances at δ 173.9 and −4.9. In addition, thermolysis of a toluene solution of **9** and $P(NEt_2)_3$ results in rapid and quantitative formation of **7b** (Scheme 8). This result can only be explained by the dissociation of PPh_3 from **9** to regenerate the $\sigma-\eta$-allenyl complex **1** and confirms that **7b** is thermodynamically favored over **9**. These subtle differences in thermodynamic properties prompted us to undertake a single-crystal X-ray structure determination of **9** to compare with that of **7b**.

Compound **9** crystallizes with two independent but essentially identical molecules in each asymmetric unit of the monoclinic cell. The molecular structure of one of these molecules is shown in Figure 8, and a selection of bond lengths and angles for both molecules is listed in Table 6. The structure clearly shows two iron atoms

Table 6. Selected Bond Distances (Å) and Angles (deg) for Compound 9

molecules (A)		molecule (B)	
Fe(1)−Fe(2)	2.6460(7)	Fe(3)−Fe(4)	2.6281(7)
Fe(1)−P(2)	2.2538(10)	Fe(3)−P(4)	2.2565(10)
Fe(2)−P(2)	2.1602(11)	Fe(4)−P(4)	2.1658(10)
Fe(2)−O(1)	1.987(2)	Fe(4)−O(2)	1.999(2)
Fe(1)−C(1)	2.166(4)	Fe(3)−C(40)	2.182(4)
Fe(1)−C(2)	2.171(4)	Fe(3)−C(41)	2.167(3)
Fe(2)−C(2)	1.962(3)	Fe(4)−C(41)	1.964(3)
C(1)−C(2)	1.415(5)	C(40)−C(41)	1.413(5)
C(2)−C(3)	1.457(5)	C(41)−C(42)	1.460(5)
C(3)−C(4)	1.343(5)	C(42)−C(43)	1.352(5)
C(4)−O(1)	1.316(4)	C(43)−O(2)	1.310(4)
C(4)−P(1)	1.803(4)	C(43)−P(3)	1.811(3)
Fe(1)−P(2)−Fe(2)	73.63(3)	Fe(4)−P(4)−Fe(3)	72.89(3)
O(1)−Fe(2)−P(2)	154.71(8)	O(2)−Fe(4)−P(4)	155.00(8)
C(1)−Fe(1)−P(2)	84.22(11)	C(40)−Fe(3)−P(4)	84.50(11)
C(2)−Fe(1)−P(2)	80.29(9)	C(41)−Fe(3)−P(4)	80.94(10)
C(1)−C(2)−Fe(2)	129.2(3)	C(40)−C(41)−Fe(4)	129.1(3)
C(3)−C(2)−Fe(2)	109.3(2)	C(42)−C(41)−Fe(4)	109.3(2)
C(2)−C(1)−Fe(1)	71.1(2)	C(41)−C(40)−Fe(3)	70.5(2)
C(3)−C(2)−Fe(1)	120.0(2)	C(42)−C(41)−Fe(3)	118.4(2)
C(1)−C(2)−Fe(1)	70.8(2)	C(40)−C(41)−Fe(3)	71.6(2)
C(1)−C(2)−C(3)	121.1(3)	C(40)−C(41)−C(42)	121.0(3)
C(4)−C(3)−C(2)	114.0(3)	C(43)−C(42)−C(41)	114.2(3)
O(1)−C(4)−C(3)	121.7(3)	O(2)−C(43)−C(42)	121.7(3)
C(4)−O(1)−Fe(2)	110.1(2)	C(43)−O(2)−Fe(4)	110.2(2)
C(3)−C(4)−P(1)	123.2(3)	C(42)−C(43)−P(3)	122.6(3)
O(1)−C(4)−P(1)	114.8(3)	O(2)−C(43)−P(3)	115.4(2)

bridged by a zwitterionic α-functionalized alkenyl ligand, σ-bonded to Fe(2) (Fe(2)−C(2) = 1.962(3) Å) and η^2-bonded to Fe(1) (Fe(1)−C(1) = 2.166(4) Å, Fe(1)−C(2) = 2.171(4) Å). As for **7b**, the β-carbon atom, C(2), is symmetrically bonded to Fe(1) (ΔFe−C = 0.005 Å), while the α-carbon is asymmetrically bound to both iron atoms (ΔFe−C = 0.209 Å). As expected, the bond length pattern within the five-membered metallacycle is similar to that in **7b** and consistent with delocalization over Fe(2), O(1), C(4), and C(3). While the bond lengths of Fe(2)−O(1), O(1)−C(4), and C(4)−C(3) are indicative of bond orders intermediate between 1 and 2, Fe(2)−C(2) is close to that expected for an Fe−C σ-interaction in a $\sigma-\pi$-vinyl complex, and the remaining endocyclic carbon−carbon bond, C(2)−C(3), corresponds to a bond order of 1. The delocalization within the metallacycle extends to the exocyclic phosphorus−carbon bond (P(1)−C(4) = 1.803(4) Å), which is slightly shorter than in triphenyl phosphine[39] and more consistent with a phosphonium salt.[38] In addition P(1) is close to tetrahedral, with most C−P−C angles close to the ideal value of 100°. As for **7b**, **9** can be considered as a α-phosphonium-alkoxide-functionalized $\sigma-\eta$-alkenyl complex, with the coordinated alkoxide forming a five-membered metallacycle and the phosphonium center attached to the carbonyl carbon.

The facile isomerization of **8** to **9** can readily be explained by the formation of a room-temperature dissociative equilibrium between $[Fe_2(CO)_6(\mu\text{-}PPh_2)(\mu\text{-}\eta^1\text{:}\eta^1\text{-}HC{=}C\{PPh_3\}CH_2)]$ (**8**) and the $\sigma-\eta$-allenyl complex $[Fe_2(CO)_6(\mu\text{-}PPh_2)\{\mu\text{-}\eta^1\text{:}\eta^2\text{-}(H)C{=}C{=}CH_2\}]$ (**1**), the latter of which undergoes phosphine−carbonyl−allenyl coupling. In contrast, we have shown that its dimetallacyclopentane counterpart $[Fe_2(CO)_6(\mu\text{-}PPh_2)\{\mu\text{-}\eta^1\text{:}\eta^1\text{-}H_2CC(NHR)CH_2\}]$ does not isomerize to the corresponding β,γ-unsaturated carbonyl derivative $[Fe_2(CO)_5(\mu$-

(39) Daly, J. J. *J. Chem. Soc.* **1964**, 3799.

Table 7. Summary of Crystal Data and Structure Determination for Compounds 2a, 3a/4a, 6a, 7b, 8, and 9

	2a	3a/4a	6b	7b	8	9
mol formula	$C_{27}H_{31}Fe_2N_3O_6P_2$	$C_{27}H_{31}Fe_2N_3O_6P_2$	$C_{32}H_{43}Fe_2N_3O_5P_2$	$C_{33}H_{43}Fe_2N_3O_6P_2$	$C_{39}H_{28}Fe_2O_6P_2 \cdot CH_2Cl_2$	$C_{39}H_{28}Fe_2O_6P_2 \cdot {}^1/_2CH_2Cl_2$
fw	667.2	667.2	723.3	751.3	851.2	808.7
cryst size, mm	0.07 × 0.15 × 0.33	0.12 × 0.30 × 0.38	0.26 × 0.32 × 0.50	0.15 × 0.33 × 0.38	0.10 × 0.24 × 0.29	0.11 × 0.14 × 0.30
temp, K	160	160	160	173	160	160
cryst syst	monoclinic	monoclinic	monoclinic	monoclinic	triclinic	monoclinic
space group	$P2_1/n$	$P2_1$	$P2_1/c$	$P\bar{1}$	$P\bar{1}$	$P2_1/n$
a, Å	11.8666(12)	9.0206(15)	18.0652(17)	16.136(4)	10.5273(13)	16.7155(8)
b, Å	16.5989(17)	16.567(3)	11.6135(11)	14.227(3)	11.3159(14)	25.7634(12)
c, Å	15.8624(16)	10.5544(17)	16.2378(14)	31.614(7)	17.517(2)	17.0192(8)
α, deg					72.776(3)	
β, deg	103.901(3)	105.853(4)	90.638(2)	95.183(6)	83.932(3)	99.635(2)
γ, deg					75.915(3)	
V, Å^3	3032.9(5)	1517.3(4)	3406.5(5)	7228(3)	1932.0(4)	7225.9(6)
Z	4	2	4	8	2	8
*D*calcd, g cm^{-3}	1.461	1.460	1.410	1.381	1.463	1.487
μ, mm^{-1}	1.106	1.105	0.988	0.936	1.018	1.013
F(000)	1376	688	1512	3136	868	3304
θ range, deg	1.94−25.00	2.01−26.00	2.08−28.38	1.91−28.86	1.93−28.86	1.87−28.88
max indices: *h*, *k*, *l*	14, 19, 18	11, 20, 12	23, 15, 21	21, 19, 42	14, 15, 23	22, 33, 22
no. of reflns measd	15 718	8667	20890	22 491	19 680	45 497
no. of unique reflns	5329	5290	7781	8578	8997	17 239
no. of reflns with $F^2 > 2\sigma(F^2)$	3759	4371	6166	6277	6248	10 514
transmission coeff range	0.696−0.894	0.557−0.862	0.751−0.862	0.731−0.862	0.680−0.930	0.708−0.894
R_{int} (on F^2)	0.0526	0.0361	0.0239	0.0351	0.0602	0.0663
weighting params[a] *a*, *b*	0.0602, 0	0.0714, 0	0.0330, 0.4430	0.0503, 0	0.0001, 51.8215	0.0470, 3.7942
R[b]	0.0458	0.0522	0.0267	0.0392	0.1097	0.0558
R_w[c]	0.1129	0.1269	0.0660	0.0963	0.3014	0.1247
no. of params	426	386	413	427	470	928
GOF[d] on F^2	0.992	1.015	1.035	1.012	1.161	1.014
max, min in diff map, e Å^{-3}	0.391, −0.439	0.829, −0.711	0.417, −0.278	0.783, −0.383	1.904, −0.950	0.849, −0.877

[a] $w^{-1} = \sigma^2(F_o^2) + (aP)^2 + bP$, where $P = (F_o^2 + 2F_c^2)/3$. [b] Conventional $R = \sum||F_o| - |F_c||/\sum|F_o|$ for "observed" reflections having $F_o^2 > 2\sigma(F_o^2)$. [c] $R_w = [\sum w(F_o^2 - F_c^2)^2/\sum w(F_o^2)^2]^{1/2}$ for all data. [d] GOF $= [\sum w(F_o^2 - F_c^2)^2/(\text{no. of unique reflns - no. of params})]^{1/2}$.

Scheme 9

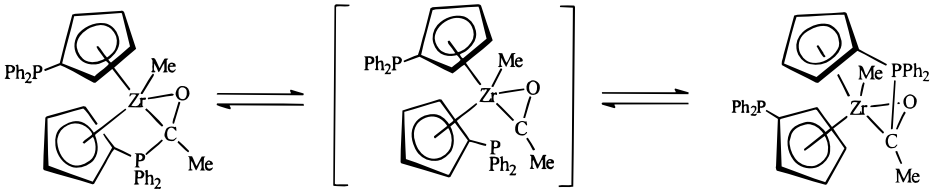

PPh$_2$)(μ-η^1:η^2-{NHRC(O)CH$_2$}C=CH$_2$)], but that these products result from competing reactions involving nucleophilic addition to C$_\beta$ and amine−carbonyl−allenyl coupling, respectively. It is not surprising that these dimetallacyclopentanes do not isomerize since the formation of an equilibrium between [Fe$_2$(CO)$_6$(μ-PPh$_2$)-{μ-η^1:η^1-H$_2$CC(NHR)CH$_2$}] and **1** would involve C−H bond activation, 1,3-H migration, and amine dissociation. The high barrier to C−H activation prevents the formation of such an equilibrium, and at elevated temperatures CO loss to give the enamine [Fe$_2$(CO)$_5$(μ-PPh$_2$){μ-η^1(C):η^2(C):η^1(N)-(H)C=CCH$_3$(NHR)}] is the dominant reaction (Scheme 5),[10a] even though [Fe$_2$(CO)$_5$-(μ-PPh$_2$)(μ-η^1:η^2-{NHRC(O)CH$_2$}C=CH$_2$)] may be the thermodynamically favored isomer. In the case of **2b**,**c** and **8**, isomerization to their thermodynamically favored zwitterionic σ−η-alkenyl counterparts **7b**,**c** and **9** is considerably more facile than decarbonylation, since the formation of an equilibrium with **1** does not require C−H activation. Surprisingly, **2a** is an exception since under conditions of thermolysis decarbonylation to give the corresponding σ−η^3-vinyl carbene **6a** is more facile than isomerization.

Closely related intramolecular dissociative equilibria between acyl and phosphonium alkoxide complexes have previously been reported by Tikkanen.[37] Rapid reversible attack of the cyclopentadienyl-substituted diphenyl phosphine in [{η^5-C$_5$H$_4$PPh$_2$}(η^5-C$_5$H$_5$)Zr{C(O)Me}X] (X = Me, Cl) at the acyl carbon leads to an equilibrium with its phosphonium alkoxide isomer [{η^5-C$_5$H$_4$PPh$_2$C-(O)Me}(η^5-C$_5$H$_5$)ZrCl] (Scheme 9).[37a] The position of this equilibrium depends on the identity of X. Similarly, the carbonylation of [{η^5-C$_5$H$_4$PPh$_2$}$_2$ZrMeCl] has been reported to give [{η^5-C$_5$H$_4$PPh$_2$}{(η^5-C$_5$H$_4$)PPh$_2$C(O)Me}-ZrCl], which results from intramolecular attack of the ring-bound diphenyl phosphine on the carbonyl carbon atom of a transient acyl complex. These products are fluxional and undergo phosphine exchange at the carbon atom of the acyl group. One proposed mechanism involves a dissociative process whereby loss of phosphine regenerates the acyl group, which is then susceptible to attack by the other phosphine.[37b] Clearly,

there are distinct similarities between the dissociative fluxional processes in these zirconium acyl complexes (Scheme 9) and the equilibrium between the dimetallacyclopentenes **2b,c** and **1**, which we suggested involves the zwitterionic phosphonium acylate derivative shown in Scheme 7.

Casey and co-workers report that in the majority of cases nucleophiles undergo kinetic addition at the central carbon of η^3-propargyl rhenium cations to give rhenacyclobutenes, and subsequent transformations lead to a variety of products.[7c] Kinetic addition of pyridine to the unsubstituted η^3-rhenium propargyl cation $[(\eta^5\text{-}C_5Me_5)(CO)_2Re(\eta^3\text{-}CH_2C{\equiv}CH)]^+$ affords the rhenacyclobutene $[(\eta^5\text{-}C_5Me_5)(CO)_2Re\{\eta^3\text{-}CH_2C(NC_5H_5){=}CH\}]$, which readily isomerizes to its η^2-allene isomer $[(\eta^5\text{-}C_5Me_5)(CO)_2Re\{\eta^3\text{-}CH_2{=}C{=}CH(NC_5H_5)\}]$ via a dissociative mechanism. In contrast, the sterically crowded *tert*-butyl-substituted η^3-propoargyl derivative $[(\eta^5\text{-}C_5Me_5)(CO)_2Re\{\eta^3\text{-}CH_2C{\equiv}CC(CH_3)_3\}]^+$ reacts with 4-(dimethylamino)pyridine to afford the corresponding rhenacyclobutene, which readily rearranges to its η^2-alkyne isomer $[(\eta^5\text{-}C_5Me_5)(CO)_2Re\{\eta^3\text{-}NC_5H_4NMe_2CH_2{=}C{=}C(CH_3)_3\}]$. Phosphorus-based nucleophiles were found to undergo a similar addition isomerization sequence.

Qualitatively, the rate of isomerization increases as the steric bulk of the phosphine increases [$P(NMe_2)_3 > P(NEt_2)_3 \approx P(N^nPr_2)_3 > PPh_3$]. While **2a** shows no sign of isomerization, the isomerization of **2b,c** is complete after 2 h in refluxing toluene, while the corresponding isomerization of **8** occurs at room temperature. As phosphine dissociation appears to be integral to this isomerization, the observed rate acceleration may be steric in origin, with larger phosphines favoring the formation of an equilibrium between the dimetallacyclopentene and **1**. Conversely, dimetallacyclopentenes formed from **1** and less bulky phosphines appear to be stable with respect to dissociation, and decarbonylation to give the vinylcarbene becomes the dominant pathway.

Conclusions

The $\sigma-\eta$-allenyl complex $[Fe_2(CO)_6(\mu\text{-}PPh_2)\{\mu\text{-}\eta^1{:}\eta^2\text{-}(H)C_\alpha{=}C_\beta{=}C_\gamma H_2\}]$ (**1**) undergoes a quantitative acid-promoted isomerization to the $\sigma-\eta$-acetylide complex $[Fe_2(CO)_6(\mu\text{-}PPh_2)\{\mu\text{-}\eta^1{:}\eta^2\text{-}C{\equiv}CH_3\}]$ (**5**) and several possible mechanisms are discussed. The isomerization of **1** into **5** provides a high-yield inexpensive and convenient route to $[Fe_2(CO)_6(\mu\text{-}PPh_2)\{\mu\text{-}\eta^1{:}\eta^2\text{-}C{\equiv}CH_3\}]$ from cheap, readily available starting materials, $[Fe_2(CO)_7(\mu\text{-}PPh_2)]Na$, propargyl bromide, and acid. Diiron $\mu\text{-}\eta^2$-acetylide complexes of this type are generally prepared from $[Fe_3(CO)_{12}]$ and $Ph_2PC{\equiv}CR$, a reaction that involves carbonyl substitution, metal fragmentation, and P−C bond cleavage, often resulting in low and unpredictable yields.[39] The reactivity of phosphorus-based nucleophiles with **5** was found to parallel that previously described by Carty and co-workers[40] and is dominated by nucleophilic addition to the α- and β-carbon atoms of the bridging acetylide to afford vinylidene- and dimetallacyclobutene-bridged complexes. In contrast, tris(dialkylamino) phosphines react with **1** via $P-C_\beta$ bond formation to give the dimetallacyclopentene derivatives $[Fe_2(CO)_6(\mu\text{-}PPh_2)(\mu\text{-}\eta^1{:}\eta^1\text{-}HC{=}C\{P(NR_2)_3\}CH_2)]$ (**2a−c**). While stable in the crystalline state, in solution **2a−c** slowly decarbonylate to give $[Fe_2(CO)_5(\mu\text{-}PPh_2)(\mu\text{-}\eta^3\text{-}C(H)C\{P(NR_2)_3\}CH_2)]$, bridged by a $\mu\text{-}\eta^3$-vinylcarbene. While **6a** is the sole product of thermolysis of **2a**, surprisingly thermolysis of **2b** gives **6b** together with a second product, identified by X-ray crystallography as $[Fe_2(CO)_5(\mu\text{-}PPh_2)\{\mu\text{-}\eta^1{:}\eta^2\text{-}(\{P(NEt_2)_3\}C(O)CH_2)C{=}CH_2\}]$ (**7b**), which contains a highly unusual α-phosphonium-alkoxide-functionalized $\sigma-\eta$-alkenyl ligand, with the coordinated alkoxide forming a five-membered metallacycle and the phosphonium center attached to the carbonyl carbon. Overall, the transformation of **2b** into **7b** corresponds to an isomerization that involves phosphine−carbonyl−allenyl coupling. The reaction between **1** and PPh_3 provides a further example of this isomerization. The kinetic product of addition to C_β, $[Fe_2(CO)_6(\mu\text{-}PPh_2)(\mu\text{-}\eta^1{:}\eta^1\text{-}HC{=}C\{PPh_3\}CH_2)]$ (**8**), rapidly and quantitatively isomerizes to $[Fe_2(CO)_5(\mu\text{-}PPh_2)\{\mu\text{-}\eta^1{:}\eta^2\text{-}PPh_3C(O)CHC{=}CH_2\}]$ (**9**), via PPh_3 dissociation followed by phosphine−carbonyl−allenyl coupling. Detailed ^{31}P NMR studies provide evidence for the formation of an equilibrium between **8** and **1**, which facilitates isomerization to the thermodynamically favored $\sigma-\eta$-alkenyl derivative **9**, the latter of which also forms a dissociative equilibrium with **1**. In contrast, the dimetallacyclopentanes $[Fe_2(CO)_6(\mu\text{-}PPh_2)\{\mu\text{-}\eta^1{:}\eta^1\text{-}H_2C{-}C(Nu)CH_2\}]$ do not isomerize since the high barrier to C−H activation prevents the formation of an equilibrium with $[Fe_2(CO)_6(\mu\text{-}PPh_2)\{\mu\text{-}\eta^1{:}\eta^2\text{-}(H)C_\alpha{=}C_\beta{=}C_\gamma H_2\}]$ (**1**), even though their isomeric β,γ-unsaturated carbonyl derivatives $[Fe_2(CO)_5(\mu\text{-}PPh_2)(\mu\text{-}\eta^1{:}\eta^2\text{-}\{NuC(O)CH_2\}C{=}CH_2)]$ may be thermodynamically favored. At elevated temperatures loss of CO gives the enamine-bridged complexes $[Fe_2(CO)_5(\mu\text{-}PPh_2)\{\mu\text{-}\eta^1(C){:}\eta^2(C){:}\eta^1(N)\text{-}(H)C{=}CCH_3(NHR)\}]$.

Experimental Section

General Procedures. Unless otherwise stated all manipulations were carried out in an inert atmosphere glovebox or by using standard Schlenk line techniques. Diethyl ether and hexane were distilled from Na/K alloy, tetrahydrofuran from potassium, and dichloromethane from CaH_2. $CDCl_3$ was predried with CaH_2, vacuum transferred, and stored over 4 Å molecular sieves. Infrared spectra were recorded on a Mattson Genesis FTIR spectrometer operating WINFIRST software. Reactions were monitored by thin-layer chromatography (Baker flex silica gel, 1B-F).Variable-temperature ^{31}P NMR spectra were recorded on a JEOL LAMBDA 500. Column chromatography was carried out with alumina purchased from Aldrich Chemical Co. and deactivated with 6% w/w water prior to loading. Tris(dialkylamino) phosphines were purchased from Aldrich Chemical Co. and used without further purification. The diiron complex $[Fe_2(CO)_6(\mu\text{-}PPh_2)\{\mu\text{-}\eta^1{:}\eta^2\text{-}(H)C{=}C{=}CH_2\}]$ was prepared as previously described.[8a]

Preparation of $[Fe_2(CO)_6(\mu\text{-}PPh_2)(\mu\text{-}\eta^1{:}\eta^1\text{-}HC{=}C\{P(NMe_2)_3\}CH_2)]$ (2a). A diethyl ether solution of $P(NMe_2)_3$ (0.065 mL, 0.4 mmol) and **1** (0.200 g, 0.4 mmol) was stirred overnight, during which time a yellow crystalline material appeared. The solvent was removed under reduced pressure to leave a yellow-orange solid residue. This residue was dissolved in the minimum amount of dichloromethane, absorbed onto deactivated alumina, dried, placed on a 300 × 30 mm alumina column, and eluted with petroleum ether/dichloromethane (60:40, v/v). The first band to elute was collected and crystallized from toluene to give **2a** as yellow

(40) Cherkas, A. A.; Randall, L. H.; MacLaughlin, S. A.; Mott, G. N.; Taylor, N. J.; Carty, A. J. *Organometallics* **1988**, *7*, 969.

crystals in 70% yield (0.185 g). IR (ν(CO), cm^{-1}, C_6H_{14}): 2038 m, 1992 s, 1973 s, 1942 m, 1928 w. $^{31}P\{^1H\}$ (202.5 MHz, $CDCl_3$, δ): 207.4 (s, μ-PPh_2), 43.9 (s, $P(NMe_2)_3$). ^1H NMR (500.1 MHz, $CDCl_3$, δ): 7.85 (d, $^3J_{PH}$ = 12.8 Hz, *H*C═C−CH_2), 7.76 (t, $^3J_{HH}$ = $^3J_{PH}$ = 7.9 Hz, 2H, C_6H_5), 7.65 (t, $^3J_{HH}$ = $^3J_{PH}$ = 8.0 Hz, 2H, C_6H_5), 7.2−7.0 (m, 6H, C_6H_5), 2.26 (d, $^3J_{PH}$ = 9.2 Hz, 18H, $P\{N(CH_3)_2\}_3$), 1.09 (t, $^3J_{PH}$ = 6.4 Hz, 2H, HC═C−CH_aH_b). $^{13}C\{^1H\}$ NMR (125.7 MHz, $CDCl_3$, δ): 224.7 (d, $^2J_{PC}$ = 33.6 Hz, *C*O), 220.4 (d, $^2J_{PC}$ = 30.0 Hz, *C*O), 216.8 (d, $^2J_{PC}$ = 27.0 Hz, *C*O), 211.5 (t, $^2J_{PC}$ = 12.0 Hz, *C*O), 190.2 (d, $^2J_{PC}$ = 18.1 Hz, H*C*═C−CH_2), 145.8 (d, $^1J_{PC}$ = 29.0 Hz, C_6H_5), 143.6 (d, $^1J_{PC}$ = 27.0 Hz, C_6H_5), 136.9 (dd, $^1J_{PC}$ = 92.0 Hz, $^3J_{PC}$ = 16.0 Hz, HC═*C*−CH_2), 134.3−127.6 (m, C_6H_5), 37.5 (br d, $^2J_{PC}$ = 7.7 Hz, $P\{N(CH_3)_2\}_3$), 17.1 (dd, $^2J_{PC}$ = 14.0 Hz, $^2J_{PC}$ = 5.7 Hz, HC═C−*C*H_2). Anal. Calcd for $C_{27}H_{31}Fe_2N_3O_6P_2$: C, 48.60; N, 6.30; H, 4.68. Found: C, 48.32; N, 6.11; H, 4.41.

Preparation of [$Fe_2(CO)_6$(μ-PPh_2)(μ-η^1:η^1-HC═C{$P(NEt_2)_3$}-CH_2)] (2b). Compound **2b** was prepared using a procedure similar to that described above for **2a** and was obtained as yellow crystals in 65% yield from toluene at room temperature. IR (ν(CO), cm^{-1}, C_6H_{14}): 2038 m, 1992 s, 1971 s, 1940 m, 1925 w. $^{31}P\{^1H\}$ (202.5 MHz, $CDCl_3$, δ): 205.6 (s, μ-PPh_2), 44.9 (s, $P(NEt_2)_3$). ^1H NMR (500.1 MHz, $CDCl_3$, δ): 7.86 (d, $^3J_{PH}$ = 13.8 Hz, *H*C═C−CH_2), 7.8−7.6 (m, 4H, C_6H_5), 7.0−7.2 (m, 6H, C_6H_5), 2.61 (m, 12H, $P\{N(CH_2CH_3)_2\}_3$), 1.15 (t, $^3J_{PH}$ = 6.4 Hz, 2H, HC═C−*C*H_2), 0.91 (t, $^3J_{HH}$ = 7.1 Hz, 18H, $P\{N(CH_2CH_3)_2\}_3$). $^{13}C\{^1H\}$ NMR (125.7 MHz, $CDCl_3$, δ): 224.5 (d, $^2J_{PC}$ = 32.9 Hz, *C*O), 220.3 (d, $^2J_{PC}$ = 26.2 Hz, *C*O), 217.3 (d, $^2J_{PC}$ = 19.4 Hz, *C*O), 212.0 (dd, $^2J_{PC}$ = 13.4 Hz, $^4J_{PC}$ = 3.4 Hz, *C*O), 211.7 (dd, $^2J_{PC}$ = 11.6 Hz, $^4J_{PC}$ = 2.5 Hz, *C*O), 187.3 (d, $^2J_{PC}$ = 17.7 Hz, H*C*═C−CH_2), 146.4 (d, $^1J_{PC}$ = 28.7 Hz, C_6H_5), 144.0 (d, $^1J_{PC}$ = 26.9 Hz, C_6H_5), 139.0 (dd, $^1J_{PC}$ = 90.3 Hz, $^3J_{PC}$ = 15.3 Hz, HC═*C*-CH_2), 134.2−127.6 (m, C_6H_5), 40.0 (d, $^2J_{PC}$ = 4.3 Hz, $P\{N(CH_2CH_3)_2\}_3$), 16.7 (dd, $^2J_{PC}$ = 14.1 Hz, $^2J_{PC}$ = 6.2 Hz, HC═C-*C*H_2), 13.6 (d, $^3J_{PC}$ = 3.0 Hz, $P\{N(CH_2CH_3)_2\}_3$). Anal. Calcd for $C_{33}H_{43}Fe_2N_3O_6P_2$: C, 52.75; N, 5.59; H, 5.77. Found: C, 52.75; N, 5.50; H, 5.88.

Preparation of [$Fe_2(CO)_6$(μ-PPh_2)(μ-η^1:η^1-HC═C-{$P(N^nPr_2)_3$}CH_2)] (2c). Following the procedure described above for the preparation of **2a**, compounds **2c** and **7c** were isolated in 45% and 25% yields, respectively, as crystalline solids from *n*-hexane. IR (ν(CO), cm^{-1}, C_6H_{14}): 2036 m, 1992 s, 1971 s, 1938 m, 1923 w. $^{31}P\{^1H\}$ (202.5 MHz, $CDCl_3$, δ): 207.0 (d, $^4J_{PP}$ = 8.5 Hz, μ-PPh_2), 46.4 (d, $^4J_{PP}$ = 8.5 Hz, $P(N^nPr_2)_3$). ^1H NMR (500.1 MHz, $CDCl_3$, δ): 7.94 (dd, $^3J_{PH}$ = 26.3 Hz, $^3J_{PH}$ = 1.6 Hz *H*C═C−CH_2), 7.7−7.6 (m, 4H, C_6H_5), 7.2−7.0 (m, 6H, C_6H_5), 2.56−2.39 (m, 12H, $P\{N(CH_2CH_2CH_3)_2\}_3$), 1.4−1.1 (m 12H, $P\{N(CH_2CH_2CH_3)_2\}_3$)), 1.06 (m, 2H, HC═C−CH_2), 0.76 (t, $^3J_{HH}$ = 7.3 Hz, 18H, $P\{N(CH_2CH_3)_2\}_3$). $^{13}C\{^1H\}$ NMR (125.7 MHz, $CDCl_3$, δ): 223.9 (d, $^2J_{PC}$ = 33.0 Hz, *C*O), 219.9 (d, $^2J_{PC}$ = 26.9 Hz, *C*O), 216.7 ($^2J_{PC}$ = 22.7 Hz, *C*O), 211.4 (m, CO), 188.0 (d, $^2J_{PC}$ = 16.6 Hz, H*C*═C−CH_2), 146.2−127.4 (m, C_6H_5), 137.2 (dd, $^1J_{PC}$ = 90.0 Hz, $^3J_{PC}$ = 15.6 Hz, HC═*C*−CH_2), 48.4 (d, $^2J_{PC}$ = 2.1 Hz, $P\{N(CH_2CH_2CH_3)_2\}_3$), 21.3 (d, $^3J_{PC}$ = 3.1 Hz, $P\{N(CH_2CH_2CH_3)_2\}_3$), 16.1 (dd, $^2J_{PC}$ = 13.4 Hz, $^2J_{PC}$ = 5.2 Hz, HC═C−*C*H_2), 11.2 (s, $P\{N(CH_2CH_2CH_3)_2\}_3$). Anal. Calcd for $C_{39}H_{55}Fe_2N_3O_6P_2$: C, 56.04; N, 5.03; H, 6.63. Found: C, 56.33; N, 5.01; H, 6.66.

Synthesis of [$Fe_2(CO)_6$(μ-PPh_2)(μ-η^1-C═C{$P(NMe_2)_3$}-CH_3] (3a) and [$Fe_2(CO)_6$(μ-PPh_2)(μ-η^1:η^1-(CH_3)C═C{$P(NMe_2)_3$})] (4a). Addition of tetrafluoroboric acid dimethyl ether (0.096 mL, 0.8 mmol) to a diethyl ether solution of **1** (0.200 g, 0.4 mmol) at −40 °C resulted in an immediate color change from yellow to deep red. The reaction mixture was stirred at −40 °C for 0.5 h and warmed to room temperature, and $P(NMe_2)_3$ was added (0.131 mL, 0.8 mmol). After the mixture was stirred overnight, the solvent was removed under reduced pressure and the oily residue dissolved in dichloromethane and absorbed onto a small amount of deactivated alumina. Column chromatography using *n*-hexane/dichloromethane as eluant gave a single major orange band, which was collected and crystallized from *n*-hexane/dichloromethane to give orange crystals of **3a** and **4a** in 66% yield (0.175 g). IR (ν(CO), cm^{-1}, C_6H_{14}): 2036 m, 1990 s, 1969 m, 1946 w, 1934 w, 1915 w. **Compound 3a**: $^{31}P\{^1H\}$ (202.5 MHz, $CDCl_3$, δ): 196.0 (s, μ-PPh_2), 34.5 (s, $P(NMe_2)_3$). ^1H NMR (500.1 MHz, $CDCl_3$, δ): 7.9−7.0 (m, 10H, C_6H_5), 2.26 (d, $^2J_{PH}$ = 9.2 Hz, 18H, $P\{N(CH_3)_2\}_3$), 2.04 (dd, $^4J_{PH}$ = 3.6 Hz, 3H, CH_3−C═C−P{N-$(CH_3)_2\}_3$). $^{13}C\{^1H\}$ NMR (125.7 MHz, $CDCl_3$, δ): 217.1−212.1 (*C*O), 200.9 (dd, $^2J_{PC}$ = 19.2 Hz, $^2J_{PC}$ = 14.7 Hz, *C*═C[P{N-$(CH_3)_2\}_3$]CH_3), 145.1−127.4 (m, C_6H_5), 111.2 (dd, $^1J_{PC}$ = 45.4 Hz, $^3J_{PC}$ = 4.5 Hz, C═*C*($P\{N(CH_3)_2\}_3$)CH_3), 38.0 (d, $^2J_{PC}$ = 4.9 Hz, $P\{N(CH_3)_2\}_3$), 30.3 (dd, $^2J_{PC}$ = 25.7 Hz, $^4J_{PC}$ = 4.9 Hz, *C*H_3C═CP$\{N(CH_3)_2\}_3$). Anal. Calcd for $C_{27}H_{31}Fe_2N_3O_6P_2$: C, 48.61; N, 6.30; H, 4.68. Found: C; 48.46; N, 6.07; H, 4.53. **Compound 4a**: $^{31}P\{^1H\}$ (202.5 MHz, $CDCl_3$, δ): 124.2 (d, $^3J_{PP}$ = 22.1 Hz, μ-PPh_2), 45.7 (d, $^3J_{PP}$ = 22.1 Hz, $P(NMe_2)_3$). ^1H NMR (500.1 MHz, $CDCl_3$, δ): 7.9−7.0 (m, 10H, C_6H_5), 2.44 (d, $^2J_{PH}$ = 9.2 Hz, 18H, $P\{N(CH_3)_2\}_3$), 2.07 (d, $^3J_{PH}$ = 3.6 Hz, 3H, C═C($P\{N(CH_3)_2\}_3$)CH_3). $^{13}C\{^1H\}$ NMR (125.65 MHz, $CDCl_3$, δ): 219.4 (dd, $^2J_{PC}$ = 15.8 Hz, $^2J_{PC}$ = 4.7 Hz, CH_3-*C*═C−P{N-$(CH_3)_2\}_3$}), 217.1−212.1 (*C*O), 145.1−127.4 (m, C_6H_5), 115.6 (dd, $^1J_{PC}$ = 142.0 Hz, $^2J_{PC}$ = 2.4 Hz, H_3C−C═*C*−$P\{N(CH_3)_2\}_3$), 38.4 (d, $^2J_{PC}$ = 11.0 Hz, $P\{N(CH_3)_2\}_3$), 37.1 (dd, $^2J_{PC}$ = 26.9 Hz, $^4J_{PC}$ = 4.9 Hz, H_3C−C═C−$P\{N(CH_3)_2\}_3$). Anal. Calcd for $C_{27}H_{31}Fe_2N_3O_6P_2$: C, 48.61; N, 6.30; H, 4.68. Found: C, 48.46; N, 6.07; H, 4.53.

Isomerization of [$Fe_2(CO)_6$(μ-PPh_2){μ-η^1:η^2-(H)C═C═CH_2}] (1). Trifluoroacetic acid (0.061 mL, 0.79 mmol) was added to a solution of **1** (0.40 g, 0.79 mmol) in dichloromethane (20 mL). After stirring for 2 h at room temperature the solvent was removed under reduced pressure to give a yellow oily residue, which was dissolved in the minimum volume of dichloromethane (1−2 mL), absorbed onto deactivated alumina, placed on a 300 × 30 mm column, and eluted with petroleum ether. The only band to elute was collected and crystallized from hexane to give **5** in 85% isolated yield (0.34 g). IR (ν(CO), cm^{-1}, C_6H_{14}): 2071 m, 2033 s, 2008 m, 1986, 1971 w. $^{31}P\{^1H\}$ (202.5 MHz, $CDCl_3$, δ): 151.5 (μ-PPh_2). ^1H NMR (500.1 MHz, $CDCl_3$, δ): 7.79−7.13 (m, 10H, C_6H_5), 1.51 (d, $^4J_{PH}$ = 10.7 Hz, 3H, CCH_3). $^{13}C\{^1H\}$ NMR (125.7 MHz, $CDCl_3$, δ): 210.0 (br, s CO), 138.8−127.6 (m, C_6H_5), 98.3 (d, $^2J_{PC}$ = 51.6 Hz, *C*≡CCH_3), 88.8 (d, $^2J_{PC}$ =7.3 Hz, C≡*C*CH_3), 9.2 (d,, $^4J_{PC}$ = 2.0 Hz, C≡C*C*H_3). Anal. Calcd for $C_{21}H_{13}$-Fe_2O_6P: C, 50.01; H, 2.60. Found: C, 49.89; H, 2.49.

Reaction of [$Fe_2(CO)_6$(μ-PPh_2){μ-η^1:η^2-(H)C═C═CH_2}] with HBF_4. Tetrafluoroboric acid diethyl ether complex (0.03 mL, 2.1 mmol) was added to a solution of **1** (0.10 g, 1.98 mmol) in chloroform (5 mL). The reaction mixture changed from yellow to deep red-purple immediately and then to an intense orange over a period of several minutes. A sample was removed from the reaction vessel, and the initial stages of the reaction were monitored by IR spectroscopy, which showed the formation of a high-frequency-shifted intermediate that was gradually replaced by ν(CO) bands associated with **5**. A similar experiment was carried out in $CDCl_3$ at −40 °C and the reaction monitored by ^1H and ^{31}P NMR spectroscopy. The intense purple coloration that appeared upon addition of acid persisted for several hours at this temperature. Spectroscopic data for intermediate **VI**: IR (ν(CO), cm^{-1}, $CDCl_3$): 2094 m, 2059 s, 2032 m, 2003 w. $^{31}P\{^1H\}$ (202.5 MHz, $CDCl_3$, δ): 36.0 (s, μ-PPh_2). ^1H NMR (400 MHz, $CDCl_3$, δ): 9.05 (d, $^2J_{PH}$ = 46.0 Hz, 1H, C*CH*), 7.1−8.0 (m, 10H, C_6H_5), 2.30 (s, 3H, CH_3).

Thermolysis of [$Fe_2(CO)_6$(μ-PPh_2)(μ-η^1:η^1-HC═C{$P(NMe_2)_3$}CH_2)] (2a). Complex **2a** (0.140 g, 0.21 mmol) was dissolved in 30 mL of toluene and the solution heated at reflux for 2 h, during which time the reaction mixture turned from yellow to bright red. The solvent was removed to give a red solid, which was dissolved in dichloromethane, absorbed onto deactivated alumina placed on a 300 × 30 mm column, and eluted with petroleum ether/dichloromethane (50:50, v/v). A single major orange/red band eluted, which was collected and

crystallized from petroleum ether/dichloromethane to give red crystals of **6a** in 75% yield (0.100 g). IR (ν(CO), cm^{-1}, C_6H_{14}): 2013 m, 1955 s, 1944 w, 1925 m, 1884 w. $^{31}P\{^1H\}$ (202.5 MHz, $CDCl_3$, δ): 145.7 (d, $^3J_{PP} = 8.0$ Hz, μ-PPh_2), 56.5 (d, $^3J_{PP} = 8.0$ Hz, $P(NMe_2)_3$). ^1H NMR (500.1 MHz, $CDCl_3$, δ): 7.79 (t, $^3J_{HH} = {}^3J_{PH} = 8.0$ Hz, 2H, C_6H_5), 7.60 (t, $^3J_{HH} = {}^3J_{PH} = 8.9$ Hz, 2H, C_6H_5), 7.17 (m, 6H, C_6H_5), 5.25 (t, $^3J_{PH} = {}^3J_{PH} = 18.0$ Hz, *H*C−C−CH_2), 2.48 (d, $^3J_{PH} = 8.9$ Hz, 18H, $P\{N(CH_3)_2\}_3$), 2.40 (d, $^3J_{PH} = 9.5$ Hz, 1H, HC≡C−CH_aH_b), 2.02 (d, $^3J_{PH} = 21.7$ Hz, 1H, HC≡C−CH_aH_b).$^{13}C\{^1H\}$ NMR (125.7 MHz, $CDCl_3$, δ): 222.1 (s, CO), 218.0 (s, *C*O), 216.5 (s, *C*O), 143.3 (d, $^1J_{PC} = 23.7$ Hz, C_6H_5), 141.7 (d, $^1J_{PC} = 25.0$ Hz, C_6H_5), 138.3 (d, $^2J_{PC} = 46.5$ Hz, H*C*−C−CH_2), 133.8−127.5 (m, C_6H_5), 94.0 (d, $^1J_{PC} = 118.9$ Hz, HC−*C*−CH_2), 37.9 (d, $^2J_{PC} = 3.1$ Hz, (P{N-$(CH_3)_2$}$_3$), 36.7 (d, $^2J_{PC} = 15.6$ Hz, HC−C−*C*H_2). Anal. Calcd for $C_{26}H_{31}Fe_2N_3O_5P_2$: C, 48.86; N, 6.57; H, 4.89. Found: C, 48.67; N, 6.43; H, 4.68.

Thermolysis of [$Fe_2(CO)_6$(μ-PPh_2)(μ-η^1:η^1-HC=C{$P(NEt_2)_3$}-CH_2)] (2b). Complex **2b** (0.040 g, 0.17 mmol) was dissolved in 30 mL of toluene and the solution heated at reflux for 2 h, during which time the reaction mixture turned from yellow to deep red. The solvent was removed to give a red solid, which was dissolved in dichloromethane absorbed onto deactivated alumina placed on a 300 × 30 mm column and eluted with *n*-hexane/dichloromethane (50:50, v/v) to give two bands. The first band to elute was collected and crystallized from *n*-hexane/dichloromethane to give **6b** as red crystals in 55% yield (0.062 g). The slower moving fraction was collected and crystallized from *n*-hexane/dichloromethane to give **7b** as red needles in 20% yield (0.026 g). **Compound 6b:** IR (ν(CO), cm^{-1}, C_6H_{14}): 2011 m, 1955 s, 1942 w, 1923 m, 1886 w. $^{31}P\{^1H\}$ (202.5 MHz, $CDCl_3$, δ): 146.0 (d, $^3J_{PH} = 34.0$ Hz, μ-PPh_2), 56.9 (d, $^3J_{PH} = 34.0$ Hz, $P(NEt_2)_3$). ^1H NMR (500.1 MHz, $CDCl_3$, δ): 7.8−7.1 (m, 10H, C_6H_5), 5.33 (t, $^3J_{PH} = {}^3J_{PH} = 17.1$ Hz, *H*C−C−CH_2), 3.67−2.78 (m, 12H, $P\{N(CH_2CH_3)_2\}_3$), 2.42 (ddd, $^3J_{PH} = 9.4$ Hz, $^3J_{PH} = 5.2$ Hz, $^2J_{HH} = 2.8$ Hz, 1H, HC≡C−CH_aH_b), 2.07 (dd, $^3J_{PH} = 21.8$ Hz, $^2J_{HH} = 2.8$ Hz, 1H, HC−C−CH_aH_b), 0.98 (t, $^3J_{HH} = 7.0$ Hz, 18H, $P\{N(CH_2CH_3)_2\}_3$).$^{13}C\{^1H\}$ NMR (125.7 MHz, $CDCl_3$, δ): 218.0 (s, *C*O), 216.9 (s, *C*O), 143.9−142.2 (m, C_6H_5), 139.0 (d, $^2J_{PC} = 45.5$ Hz, H*C*−C−CH_2), 134.2−127.8 (m, C_6H_5), 95.3 (d, $^1J_{PC} = 114.8$ Hz, HC-*C*−CH_2), 40.3 (d, $^2J_{PC} = 3.1$ Hz, $P\{N(CH_2CH_3)_2\}_3$), 38.3 (d, $^2J_{PC} = 15.5$ Hz, HC−C−*C*H_2), 13.3 (d, $^3J_{PC} = 2.1$ Hz, $P\{N(CH_2CH_3)_2\}_3$). Anal. Calcd for $C_{32}H_{43}Fe_2N_3O_5P_2$: C, 53.11; N, 5.80; H, 5.99. Found: C, 52.95; N, 5.68; H, 5.64. **Compound 7b**: IR (ν(CO), cm^{-1}, C_6H_{14}): 2015 w, 1981 s, 1948 m, 1934 w, 1913 m. $^{31}P\{^1H\}$ (32.4 MHz, $CDCl_3$, δ): 160.9 (s, μ-PPh_2), 36.8 (s, $P(NEt_2)_3$). ^1H NMR (500.1 MHz, $CDCl_3$,δ): 7.5−7.0 (m, 10H, C_6H_5), 6.70 (s, H_2C−C−C*H*−C(O)), 3.55 (d, $^3J_{PH} = 11.3$ Hz, H_aH_bC−C−CH−C(O)), 3.01 (t, $^3J_{HH} = {}^3J_{PH} = 4.5$ Hz, 12H, $P\{N(CH_2CH_3)_2\}_3$), 1.69 (d, $^3J_{PH} = 8.0$ Hz, H_aH_bC−C−CH−C(O)), 1.09 (t, $^3J_{HH} = 7.0$ Hz, 18H, $P\{N(CH_2CH_3)_2\}_3$). $^{13}C\{^1H\}$ NMR (125.7 MHz, $CDCl_3$, δ): 219.3 (d, $^2J_{PC} = 14.2$ Hz, *C*O), 216.6 (s, 3 *C*O), 215.2 (d, $^2J_{PC} = 14.3$ Hz, *C*O), 167.2 (d, $^2J_{PC} = 23.7$ Hz, H_2C−*C*−CH−C(O)), 160.6 (d, $^1J_{PC} = 159.1$ Hz, H_2C−C−CH−*C*(O)), 142.4−127.2 (m, C_6H_5), 133.6 (dd, $^2J_{PC} = 51.0$ Hz, $^2J_{PC} = 7.1$ Hz, H_2C−C−*C*H−C(O)), 54.8 (d, $^2J_{PC} = 6.5$ Hz, H_2C−C−CH−C(O)), 40.1 (d, $^2J_{PC} = 4.1$ Hz, (P{N(*C*$H_2CH_3)_2\}_3$), 13.7 (d, $^3J_{PC} = 1.8$ Hz, $(P\{N(CH_2CH_3)_2\}_3$). Anal. Calcd for $C_{33}H_{43}Fe_2N_3O_6P_2$: C, 52.75; N, 5.59; H, 5.77. Found: C, 52.93; N, 5.69; H, 5.89.

Thermolysis of [$Fe_2(CO)_6$(μ-PPh_2)(μ-η^1:η^1-HC=C{$P(N^nPr_2)_3$}CH_2)] (2c). Thermolysis as for **2b** above gave yellow crystals of **6c** in 35% yield and red crystals of **7c** in 35% yield. **Compound 6c:** IR (ν(CO), cm^{-1}, C_6H_{14}): 2011 m, 1955 s, 1940 w, 1921 m, 1886 w. $^{31}P\{^1H\}$ (202.5 MHz, $CDCl_3$, δ): 149.2 (d, $^3J_{PP} = 12.8$ Hz, μ-PPh_2), 56.7 (d, $^3J_{PP} = 12.8$ Hz, $P(N^iPr_2)_3$). ^1H NMR (500.1 MHz, $CDCl_3$, δ): 7.8−7.7 (m, 2H, C_6H_5), 7.6−7.6 (m, 2H, C_6H_5) 7.2−7.1 (m, 6H, C_6H_5), 5.5 (dt, $^3J_{PH} = 2.8$ Hz, $^3J_{PH} = 16.5$ Hz, *H*C−C−CH_2), 2.8−2.6 (m, 12H, $P\{N(CH_2CH_2CH_3)_2\}_3$), 2.34 (dt, $^3J_{PH} = {}^2J_{HH} = 2.8$ Hz, $^3J_{HH} = 8.8$ Hz, 1H, HC−C−C(H)*H*), 2.05 (dd, $^3J_{PH} = 20.8$ Hz, $^2J_{HH} = 2.8$ Hz, 1H, HC−C−C(*H*)H), 1.5−1.3 (m, 12H, $P\{N(CH_2CH_2CH_3)_2\}_3$), 0.73 (t, $^3J_{HH} = 7.3$ Hz, 18H, $P\{N(CH_2CH_2CH_3)_2\}_3$). $^{13}C\{^1H\}$ NMR (125.7 MHz, $CDCl_3$, δ): 223.7 (br d, $^2J_{PC} = 5.9$ Hz, *C*O), 219.9 (dd, $^2J_{PC} = 14.9$ Hz, $^2J_{PC} = 5.9$ Hz, *C*O), 216.9 (d, $^2J_{PC} = 2.4$ Hz, *C*O), 142.4−127.7 (m, C_6H_5), 138.6 (d, $^2J_{PC} = 45.5$ Hz, H*C*−C−CH_2), 95.0 (d, $^1J_{PC} = 113.6$ Hz, HC−*C*−CH_2), 48.9 (d, $^2J_{PC} = 2.1$ Hz, $(P\{N(CH_2CH_2CH_3)_2\}_3$), 37.8 (d, $^2J_{PC} = 13.4$ Hz, HC−C−*C*H_2), 21.7 (d, $^3J_{PC} = 3.1$ Hz, $(P\{N(CH_2CH_2CH_3)_2\}_3$), 11.3 (s, $(P\{N(CH_2CH_2CH_3)_2\}_3$). Anal. Calcd for $C_{38}H_{55}Fe_2N_3O_5P_2$: C, 56.50; N, 5.20; H, 6.87. Found: C, 56.72; N, 5.22; H, 6.90. **Compound 7c**: IR (ν(CO), cm^{-1}, C_6H_{14}): 2017 w, 1981 s, 1948 m, 1938 w, 1911 m. $^{31}P\{^1H\}$ (121.5 MHz, $CDCl_3$, δ): 161.9 (d, $^5J_{PP} = 6.7$ Hz, μ-PPh_2), 36.7 (d, $^5J_{PP} = 6.7$ Hz, $P(N^nPr_2)_3$). ^1H NMR (500.1 MHz, $CDCl_3$, δ): 7.6−7.0 (m, 10H, C_6H_5), 6.71 (s, 1H, H_2C−C−C*H*−C(O)), 3.54 (dd, $^3J_{PH} = 11.3$ Hz, $^5J_{PH} = 2.1$ Hz, 1H, H_aH_bC−C−CH−C(O)), 2.84 (quartet, $^3J_{HH} = {}^3J_{PH} = 10.1$ Hz, 12H, $P\{N(CH_2CH_2CH_3)_2\}_3$), 1.69 (br d, $^3J_{PH} = 7.0$ Hz, 1H, H_aH_bC−C−CH−C(O)), 1.48 (sept, $^3J_{HH} = 8.0$ Hz, 12H, $P\{N(CH_2CH_2CH_3)_2\}_3$), 1.19 (t, $^3J_{HH} = 7.0$ Hz, 18H, $P\{N(CH_2CCH_2CH_3)_2\}_3$). $^{13}C\{^1H\}$ NMR (125.7 MHz, $CDCl_3$, δ): 219.5 (d, $^2J_{PC} = 15.5$ Hz, *C*O), 219.5 (br s, *C*O), 216.6 (d, $^2J_{PC} = 19.1$ Hz, *C*O), 167.8 (t, $^2J_{PC} = {}^2J_{PC} = 23.7$ Hz, H_2C−*C*−CH−C(O)), 160.5 (d, $^1J_{PC} = 157.1$ Hz, H_2C−C−CH−*C*(O)), 142.5−127.4 (m, C_6H_5), 137.3 (dd, $^2J_{PC} = 51.0$ Hz, $^2J_{PC} = 7.1$ Hz, H_2C−C−*C*H−C(O)), 54.8 (s, H_2C−C−CH−C(O)), 48.7 (d, $^2J_{PC} = 3.1$ Hz, $(P\{N(CH_2CH_2CH_3)_2\}_3$), 22.0 (d, $^2J_{PC} = 2.1$ Hz, $(P\{N(CH_2CH_2CH_3)_2\}_3$), 11.5 (s, $(P\{N(CH_2CH_2CH_3)_2\}_3$). Anal. Calcd for $C_{39}H_{55}Fe_2N_3O_6P_2$: C, 56.05; N, 5.03; H, 6.64. Found: C, 55.90; N, 5.00; H, 6.87.

Preparation of [$Fe_2(CO)_6$(μ-PPh_2){μ-η^1:η^1-HC=C(PPh_3)-CH_2}] (8). A diethyl ether solution of PPh_3 (0.065 mL, 0.4 mmol) and **1** (0.200 g, 0.4 mmol) was stirred for 3 h, after which time the solvent was removed to leave a solid yellow residue. This residue was extracted into a small volume (∼1 mL) of dichloromethane, absorbed onto deactivated alumina, dried, placed on a 300 × 30 mm alumina column, and eluted with petroleum ether/dichloromethane (60:40, v/v). A fast moving yellow band eluted and was collected and crystallized from dichloromethane/hexane to give **8** as yellow crystals in 67% yield. IR (ν(CO), cm^{-1}, C_6H_{14}): 2033 s, 1986 s, 1963 m, 1938 w, 1918 w. $^{31}P\{^1H\}$ (202.5 MHz, $CDCl_3$, δ): 207.8 (d, $^4J_{PP} = 10.1$ Hz, μ-PPh_2), 7.8 (d, $^4J_{PP} = 10.1$ Hz, PPh_3). ^1H NMR (500.1 MHz, $CDCl_3$, δ): 7.90 (d, (d, $^3J_{PH} = 27.2$ Hz, *H*C=CCH_2), 7.7−7.0 (m, 25H, C_6H_5), 1.2 (m, 2H, HC=C=C*H*$_2$). $^{13}C\{^1H\}$ NMR (125.7 MHz, $CDCl_3$, δ): 223.7 (d, $^2J_{PC} = 31.5$ Hz, CO), 219.8 (d, $^2J_{PC} = 25.3$ Hz, CO), 216.3 (d, $^2J_{PC} = 56.3$ Hz, CO), 211.4 (m, CO) 180.4 (d, $^2J_{PC} = 4.6$ Hz, H_2CCCH),), 145.5−118.3 (m, C_6H_5), 141.0 (d, $^1J_{PC} = 55.3$ Hz, H_2CCCH) 18.5 (dd, $^2J_{PC} = 14.4$ Hz, $^2J_{PC} = 5.2$ Hz, H_2CCCH). Anal. Calcd for $C_{39}H_{28}Fe_2O_6P_2$: C, 61.10; H, 3.66. Found: C, 61.38; H, 3.77.

Isomerization of [$Fe_2(CO)_6$(μ-PPh_2){μ-η^1:η^1-HC=C(PPh_3)-CH_2}] (8). A diethyl ether solution of **8** (0.120 g 0.16 mmol) was stirred at room temperature for 1 h, during which time the reaction mixture turned from yellow to deep red-orange. The solvent was then removed to leave a solid orange residue, which was purified by column chromatography, using deactivated alumina support and hexane/dichloromethane (60:40, v/v) as eluant. The first yellow band to elute was collected and identified as unreacted **8**, by comparison of its IR spectrum with that reported above. The major slower moving red band was collected and crystallized from dichloromethane/hexane to give deep orange crystals of **9** in 82% yield (0.250 g). IR (ν(CO), cm^{-1}, C_6H_{14}): 2017 w, 1984 s, 1952 m, 1923 w, 1917 m. $^{31}P\{^1H\}$ (202.5 MHz, $CDCl_3$, δ): 162.7 (d, $^4J_{PP} = 5.5$ Hz, μ-PPh_2), 1.6 (d, $^4J_{PP} = 5.5$ Hz, PPh_3). ^1H NMR (500.1 MHz, $CDCl_3$, δ): 7.6−7.0 (m, 25H, C_6H_5), 6.40 (dd, $^3J_{PH} = 3.3$ Hz, $^4J_{HH} = 2.1$ Hz, H_2C=CC*H*), 3.44 (d, $^3J_{PH} = 11.2$ Hz, $^4J_{HH} = 2.1$ Hz, H_aH_bCCCH), 1.69 (br d, $^3J_{PH}$, 8.0 Hz, H_aH_bCCCH). $^{13}C\{^1H\}$ NMR (125.7 MHz, $CDCl_3$, δ): 219.1 (d, $^2J_{PC} = 15.5$ Hz, CO), 216.4 (s, CO), 214.7 (d, $^2J_{PC} = 15.5$ Hz, CO), 164.5 (dd, $^2J_{PC} = 24.8$ Hz, $^3J_{PC} = 20.6$ Hz, H_2CCCH), 153.2 (d, $^1J_{PC}$

= 93.1 Hz, HC*C*O), 141.1−127.3 (m C_6H_5), 133.6 (d, $^2J_{PC}$ = 22.7 Hz, H_2CC*C*H), 56.2 (d, $^2J_{PC}$ = 7.3 Hz, H_2*C*CCH). Anal. Calcd for $C_{39}H_{28}Fe_2O_6P_2.0.5CH_2Cl_2$: C, 58.66; H, 3.61. Found: C, 58.76; H, 3.48.

Crystal Structure Determination of 2a, 3a/4a, 6b, 7b, 8, and 9. All measurements were made on a Bruker AXS SMART CCD area-detector diffractometer using Mo Kα radiation (λ = 0.71073) and narrow frame exposures (0.3° in ω). Cell parameters were refined from the observed ω angles of all strong reflections in each data set. Intensities were corrected semiempirically for absorption, based on symmetry-equivalent and repeated reflections. No significant intensity decay was observed. The structures were solved by direct methods and refined on F^2 values for all unique data by full-matrix least-squares. Table 6 gives further details. All non-hydrogen atoms were refined anisotropically. H atoms, located in difference maps, were constrained with a riding model except for those attached to C(1) and C(3) in **6b**, C(1) in **7b**, and C(1), C(3), C(40) and C(42) in **9**, which had their coordinates freely refined because of nonstandard geometry; U(H) was set at 1.2 (1.5 for methyl groups) times U_{eq} for the parent atom. Two-fold, approximately 50/50, disorder was successfully modeled with restraints on anisotropic displacement parameters and geometry for the three NMe_2 groups in **2a**. Similar restraints were applied to atoms P(1), C(1), C(2), C(3), C(1A), and C(2A) in the co-crystallized structure of **3a**/**4a**. Programs used were SHELXTL[42a] for structure solution, refinement, and molecular graphics, Bruker AXS SMART (control) and SAINT (integration), and local programs.[42b]

Acknowledgment. We thank the University of Newcastle upon Tyne for financial support, the Nuffield Foundation and The Royal Society for grants (S.D.), and the EPSRC for funding for a diffractometer (W.C.). Our sincere thanks to Dr. Graeme Hogarth for help with NMR and valuable discussions.

Supporting Information Available: For **2a**, **3a/4a**, **6b**, **7b**, **8**, and **9** details of structure determination, non-hydrogen atomic positional parameters, full listings of bond distances and angles, anisotropic displacement parameters, and hydrogen atomic coordinates. This material is available free of charge via the Internet at http://pubs.acs.org. Observed and calculated structure factor tables are available from the authors upon request.

OM980757N

(41) (a) Blenkiron, P.; Enright, G. D.; Taylor, N. J.; Carty, A. J. *Organometallics* **1996**, *15*, 2855. (b) Cherkas, A. A.; Randall, L. H.; Taylor, N. J.; Mott, G. N.; Yule, J. E.; Guinamant, J. L.; Carty, A. J. *Organometallics* **1990**, *9*, 1677, and references therein. (c) Cherkas, A. A.; Taylor, Carty, A. J. *J. Chem. Soc., Chem. Commun.* **1990**, 385. (d) Breckenridge, S. M.; MacLaughlin, S. A.; Taylor, N. J.; Carty, A. J. *J. Chem. Soc., Chem. Commun.* **1991**, 1718. (e) Nucciarone, D.; Taylor, N. J.; Carty, A. J. *Organometallics* **1986**, *5*, 1179. (f) Nucciarone, D.; MacLaughlin, S. A.; Taylor, N. J.; Carty, A. J. *Organometallics* **1988**, *7*, 106.

(42) (a) Sheldrick, G. M. *SHELXTL user manual*, version 5; Bruker AXS Inc.: Madison, WI, 1994. (b) SMART and SAINT software for CCD diffractometers; Bruker AXS Inc.: Madison, WI, 1994.